The Data-Driven δ-Generalized Labeled Multi-Bernoulli Tracker for Automatic Birth Initialization

Keith A. LeGrand[a] and Kyle J. DeMars[b]

[a]Sandia National Laboratories, Albuquerque, NM, 87123-3453 USA
[b]Missouri University of Science and Technology, Rolla, MO, 65409-0050 USA

ABSTRACT

The δ-generalized labeled multi-Bernoulli (δ-GLMB) tracker is the first multiple hypothesis tracking (MHT)-like tracker that is provably Bayes-optimal. However, in its basic form, the δ-GLMB provides no mechanism for adaptively initializing targets at their first appearance from unlabeled measurements. By introducing a new multitarget likelihood function that accounts for new target appearance, a data-driven δ-GLMB tracker is derived that automatically initializes new targets in the tracker measurement update. Monte Carlo results of simulated multitarget tracking problems demonstrate improved multitarget tracking accuracy over comparable adaptive birth methods.

1. INTRODUCTION

Multitarget filtering is the process of simultaneously estimating one or more target's kinematic states using noisy, unattributed measurements with the possibility of misdetection and non-target-originated measurements, or clutter. There are, in general, three main approaches to multitarget tracking: joint probabilistic data association (JPDA),[1] MHT,[2] and finite set statistics (FISST).[3,4] The FISST approach has received significant attention over the past decade because it enables a top-down Bayesian approach to solving multitarget tracking problems. Central to the FISST approach is the concept of the random finite set (RFS). An RFS is a random-valued set, of which the number of elements is also random. In the FISST framework, RFSs are used to describe the collection of individual target states as well as the collection of unordered measurements at a given time step. By defining a set-valued multitarget state and set-valued multitarget measurement, FISST extends familiar concepts from single-target tracking to the multitarget domain. The resulting FISST toolset, which defines multitarget density and likelihood functions, enables solution of multitarget tracking problems using similar techniques found in single-target Bayesian estimation.

Two notable filters to emerge from the FISST approach are the probability hypothesis density (PHD)[5,6] and cardinalized probability hypothesis density (CPHD)[7] filters, which operate on a first-moment approximation of the multitarget density and admit both Gaussian mixture (GM) and sequential Monte Carlo (SMC) implementations. Unlike traditional trackers, which, generally speaking, consist of a data association step followed by a single-target filtering step, the PHD and CPHD filters avoid the data association step altogether by neglecting target identity. For applications where target identity is not important, the reduced computational complexity of unlabeled multitarget filters makes them appealing options over traditional data-association based trackers.

The PHD and CPHD filters maintain no record of track identity and, as a consequence, often suffer from track continuity issues. To alleviate this, labeled extensions were developed for the PHD filter[8,9] and CPHD filter.[10] Although these and other works improved track continuity through track labeling techniques, the concept of the *labeled RFS* was only first introduced years later in Reference 11.

Enabled by labeled RFS theory, the δ-GLMB tracker was introduced as an analytic solution to the Bayes multitarget filter.[12,13] The δ-GLMB tracker is arguably one of the most significant advancements to multitarget tracking in recent years, as it is the first MHT-like tracker that is provably Bayes-optimal.[4] The δ-GLMB tracker is a major departure from its PHD and CPHD predecessors in a number of ways. Firstly, rather than operating on a moment approximation, the δ-GLMB maintains a full multitarget density representation—a complete statistical description from which lower dimensional statistics (such as the PHD) may be computed. Secondly, a unique discrete label state is appended to the individual kinematic target state to facilitate target identification. Data association is required, but its combinatorial output can be controlled through various sampling and truncation

techniques. Lastly, target labels in the δ-GLMB filter enable a clear connection between a given target and its spatial uncertainty. This addresses a significant limitation of unlabeled representations, in which the individual contributions of targets to the consolidated uncertainty representation (namely, the unlabeled PHD) are often indistinguishable, as illustrated in Figure 1. Isolating an individual target's uncertainty in an unlabeled density

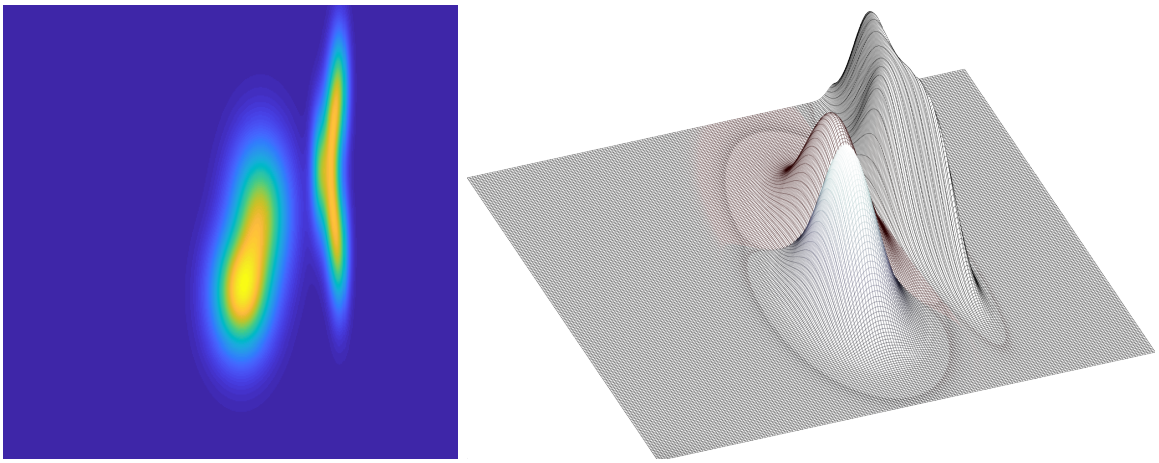

Figure 1: In an unlabeled PHD representation (left), the uncertainty associated with an individual target is often inextricable. Labeled statistics, such as the labeled PHD (right), are readily computable from the δ-GLMB filter, thereby enabling track-specific uncertainty representation. As revealed in the labeled PHD (right), three distinct targets are tracked—a feature that is not readily apparent from the unlabeled equivalent (left).

is especially challenging or impossible in situations involving closely spaced targets, low measurement signal-to-noise ratio (SNR), or high clutter rates.

A critically important but often overlooked consideration in operational multitarget tracking is the method by which target appearance, often referred to in tracking literature as target birth, is handled. In traditional tracking algorithms, such as MHT and joint integrated probabilistic data association (JIPDA),[14] new targets are initialized directly from measurement data. In RFS-based filters, however, new targets are modeled by intensity or density functions. Two challenges arise with this approach: determining an appropriate function that accurately describes the birth process and modeling that function in a computationally efficient manner.

Unlabeled birth models commonly used in RFS filters include the Poisson density,[6,15] the independently and identically distributed (i.i.d.) cluster density,[7] and the multi-Bernoulli (MB) density.[16] The Poisson density is appealing in tracking applications where little information about the birth process is known *a priori*, as the Poisson density is fully described by its intensity function (PHD).[15] The intensity function describes the spatial distribution of targets, and its integral over the scene volume is equal to the expected number of new targets, which is Poisson-distributed. The i.i.d. cluster density relaxes the Poisson-distributed cardinality assumption and instead uses an arbitrary probability mass function (pmf) to describe target cardinality. This approach is more flexible to incorporating external information about target cardinality, such as soft data from a human operator on the loop. The MB density is represented in terms of individual (single) target densities and probabilities of existence. Using an MB birth model shifts the focus to individual birth targets, as opposed to the other two aforementioned birth models, which can be interpreted as more population-centric approaches.

The generalized labeled multi-Bernoulli (GLMB) density is the most versatile labeled birth model. In fact, its available level of specificity is rarely needed to describe the limited information known about a birth process *a priori*. Two special cases of the GLMB density, namely the labeled multi-Bernoulli (LMB) density and labeled Poisson density, require less specificity and simplify the Bayes recursion. The GLMB filter is capable of accepting a GLMB birth density, but the majority of the literature has focused on the LMB density.[12,13,17,18] The LMB density is parameterized by a set of value pairs $(r^{(i)}, p^{(i)})$, in which $r^{(i)}$ represents the probability of existence of target i and $p^{(i)}$ is its density. In the context of target birth, representation in this form requires *a priori*

specification of the probability density and probability of existence on an individual target basis. Such specificity is achievable in tracking scenarios with known target birth locations and patterns, such as tracking vehicles emerging from a tunnel during heavy traffic. However, in many tracking scenarios, when far less information is known *a priori*, the LMB birth model approach may prove cumbersome or intractable.

In most real-world applications, a data-driven approach—that is, an approach where new targets are instantiated from measurement data—is advantageous, and in many cases, unavoidable. Ideally, to instantiate new targets from measurement data, only detections originating from new targets should be used to instantiate target births. Of course, the challenge is differentiating new target detections from persistent (that is, previously detected) target detections and clutter. Some insight can be gained by looking at the likelihood agreement of measurements to persistent target estimates; measurements with a strong likelihood agreement to persistent target estimates are less likely to have originated from a new target. Given a single multitarget measurement, new target measurements and clutter are indistinguishable unless their spatial densities are disjoint. To that end, most approaches[19–21] to the data-driven birth problem rely on deferred decision, that is, delaying the initialization of birth by one or more time steps.

Reference 19 provides a straightforward solution for adaptively introducing new targets from measurement data in a Bernoulli filter by sampling the birth distribution at the locations of the measurements at the previous step. Then, intuitively, a new target track is likely to be "confirmed" if another measurement is received close to a measurement at the previous time step, whereas the possibility of subsequent clutter measurements mimicking a new track is less likely. Reference 20 presents an adaptive birth model for the cardinality-balanced multi-object multi-Bernoulli (CBMeMBer) filter. The received measurements at time k are used to adaptively form the MB density of new births at time $k+1$. In an effort to minimize the bias introduced by doubly using the measurement data in both the update of persistent targets and formation of the birth density, the birth targets seeded from measurements that have strong likelihood agreement to persistent target estimates are assigned a lower probability of existence. Furthermore, an additional heuristic is introduced that prohibits new targets from being assigned a probability of existence higher than a user-specified maximum value. The same approach is applied in Reference 21 for the GLMB tracker. This approach is simple, effective, and requires minimal implementation modifications. However, this approach violates the fundamental assumption that each target generates observations independent of one another, as a birth target can be initialized from the same measurement used to update a persistent target in the same hypothesis.

The filter proposed herein addresses some of the key challenges faced when implementing the GLMB trackers on real-world data. First, a labeled Poisson RFS is used to model target birth, which requires less *a priori* knowledge and is thus more "operator-friendly." Second, to make the birth process "data-driven," the GLMB tracker is rederived such that no target may exist without a seed measurement. To achieve this, the case of undetected birth targets is ignored, and the birth process is modeled in the update stage rather than the prediction stage. The resulting filter initializes new targets immediately upon first detection with an appropriate probability of existence without introducing statistical bias or additional heuristics.

2. BACKGROUND

Throughout this work, single-target states are represented by lowercase letters (e.g. x, $\mathbf{x}$), while multitarget states are represented by uppercase letters (e.g. X, $\mathbf{X}$). Bolded symbols (e.g. $\boldsymbol{\pi}$, $\mathbf{x}$, $\mathbf{X}$) are used to distinguish labeled states and functions from unlabeled ones. Spaces are represented by blackboard bold symbols (e.g. $\mathbb{X}$, $\mathbb{Z}$, $\mathbb{L}$).

The inner product $\int f(x)g(x)\mathrm{d}x$ is denoted by $\langle f, g\rangle$ and the multitarget exponential notation defined by $f^{\mathbf{A}} \triangleq \prod_{\mathbf{a}\in\mathbf{A}} f(\mathbf{a})$, where $f^{\emptyset} \triangleq 1$ by definition, is used throughout. The Kronecker delta is generalized to handle vectors and sets as

$$\delta_A(B) = \begin{cases} 1, & \text{if } B = A \\ 0, & \text{otherwise} \end{cases}.$$

Similarly, the indicator function is defined as

$$1_A(B) = \begin{cases} 1, & \text{if } B \subseteq A \\ 0, & \text{otherwise} \end{cases}.$$

2.1 Random Finite Set

An RFS X on a space $\mathbb{X}$ is a set-valued random variable with realizations in the space of all finite subsets of $\mathbb{X}$, or $\mathcal{F}(\mathbb{X})$. A labeled RFS $\mathbf{X}$ is an RFS on $\mathbb{X} \times \mathbb{L}$, where $\mathbb{X}$ is the kinematic space and $\mathbb{L}$ is the discrete label space. The label of a labeled state $\mathbf{x}$ is recovered by $\mathcal{L}(\mathbf{x})$, where $\mathcal{L} : \mathbb{X} \times \mathbb{L} \to \mathbb{L}$ is the projection defined by $\mathcal{L}((x, \ell)) \triangleq \ell$. Similarly, for labeled RFSs, $\mathcal{L}(\mathbf{X}) \triangleq \{\mathcal{L}(\mathbf{x}) : \mathbf{x} \in \mathbf{X}\}$. The cardinality of an RFS X is denoted by $|X|$.

2.2 Generalized Labeled Multi-Bernoulli

A GLMB density can be written as a mixture of multitarget exponentials in the form[12]

$$\boldsymbol{\pi}(\mathbf{X}) = \Delta(\mathbf{X}) \sum_{\xi \in \Xi} w^{(\xi)}(\mathcal{L}(\mathbf{X}))[p^{(\xi)}]^{\mathbf{X}}, \tag{1}$$

where each $\xi \in \Xi$ represents a history of measurement association maps, each $p^{(\xi)}(\cdot, \ell)$ is a probability density on $\mathbb{X}$, and each weight $w^{(\xi)}$ is non-negative with $\sum_{(I,\xi) \in \mathcal{F}(\mathbb{L}) \times \Xi} w^{(\xi)}(I) = 1$. The distinct label indicator $\Delta(\mathbf{X}) = \delta_{(|\mathbf{X}|)}(|\mathcal{L}(\mathbf{X})|)$ ensures that only sets with distinct labels are considered. The sum of the weights $\sum_{(I,\xi) \in \mathcal{F}(\mathbb{L}) \times \Xi} w^{(\xi)}(I) 1_I(\ell)$ can be interpreted as the probability of existence for track ℓ.

2.3 δ-Generalized Labeled Multi-Bernoulli

A δ-GLMB density is a special case of the GLMB density, given by

$$\boldsymbol{\pi}(\mathbf{X}) = \Delta(\mathbf{X}) \sum_{(I,\xi) \in \mathcal{F}(\mathbb{L}) \times \Xi} \omega^{(I,\xi)} \delta_I(\mathcal{L}(\mathbf{X}))[p^{(\xi)}]^{\mathbf{X}},$$

where

$$\omega^{(I,\xi)} \triangleq w^{(\xi)}(I).$$

Two important statistics, namely the cardinality distribution $\rho(\cdot)$ and PHD $v(\cdot)$, can be recovered from the δ-GLMB density by

$$\rho(n) = \sum_{(I,\xi) \in \mathcal{F}_n(\mathbb{L}) \times \Xi} \omega^{(I,\xi)}$$
$$v(x) = \sum_{(I,\xi) \in \mathcal{F}(\mathbb{L}) \times \Xi} \sum_{\ell \in I} \omega^{(I,,\xi)} p^{(\xi)}(x, \ell),$$

where $\mathcal{F}_n(\mathbb{L})$ denotes the class of finite subsets of $\mathbb{L}$ with exactly n elements.[13]

3. DATA-DRIVEN GLMB OVERVIEW

In the data-driven GLMB, the target birth process is modeled as a Poisson RFS, new targets are defined as "born" at their first detection, and the incorporation of birth targets occurs in the measurement update. At a given time k, birth targets are defined as the subset of targets whose first detection occurred at the current time k. Targets are considered "persistent" if their first detection occurred at any time prior to the current time k. Variables and densities corresponding to birth targets and persistent targets are denoted by subscripts "b" and "p," respectively.

For a given persistent multitarget state $\mathbf{X}_\mathrm{p}$, each single-target element $(x, \ell) \in \mathbf{X}_\mathrm{p}$ is either detected with probability $p_D(x, \ell)$ or misdetected with probability $1 - p_D(x, \ell)$. Similar to References 22 and 23, a target's birth is treated here as its first detection, such that every element (x, ℓ) of a given birth multitarget state $\mathbf{X}_\mathrm{b}$ is detected with probability $p_D(x, \ell) = 1$.

A measurement association map θ is a one-to-one function that uniquely maps persistent target tracks to the incoming measurement set Z. In a given association map, the subset of measurements assigned to persistent targets is denoted by Z_θ. The association map *space* is the set of all such association maps and is denoted by Θ. Given an association map θ, another level of data association may be performed, mapping birth target tracks to the non-assigned measurements $Z_{\overline{\mathrm{p}}} = Z - Z_\theta$ via the birth measurement association map ϑ. The birth measurement association map *space* is the set of all birth measurement association maps and is denoted by V. Both θ and ϑ obey the identity that $\theta(i) = \theta(i') > 0$ or $\vartheta(i) = \vartheta(i') > 0$ implies that $i = i'$.

The filter structure of the data-driven GLMB incorporates the birth process in the update stage rather than in the prediction stage, as shown in Figure 2. At time k, the density of persistent targets $\boldsymbol{\pi}_{\mathrm{p}}(\mathbf{X}_{\mathrm{p}}|Z_{0:k-1}) = \boldsymbol{\pi}_{\mathrm{p}}(\mathbf{X}_{\mathrm{p}})$,

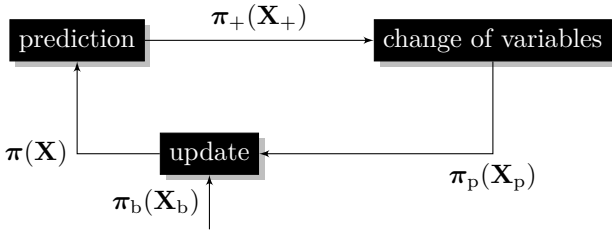

Figure 2: Block diagram of the data-driven δ-GLMB.

where $Z_{0:k-1}$ denotes all received measurements up to and including time $k-1$, and the density of new targets $\boldsymbol{\pi}_{\mathrm{b}}(\mathbf{X}_{\mathrm{b}})$ undergo a Bayes measurement update to produce the joint posterior density at time $k+1$, denoted by $\boldsymbol{\pi}(\mathbf{X} = \mathbf{X}_{\mathrm{p}} \cup \mathbf{X}_{\mathrm{b}}|Z_{0:k}) = \boldsymbol{\pi}(\mathbf{X})$. After each update, the persistent target label space $\mathbb{L}$ is redefined to include the birth target label space $\mathbb{B}$ at that update; i.e. $\mathbb{L} \triangleq \mathbb{L} \cup \mathbb{B}$. In the prediction stage, the posterior density $\boldsymbol{\pi}(\mathbf{X})$ undergoes a time-update to produce the prior density $\boldsymbol{\pi}_+(\mathbf{X}_+)$. At the next update at time $k+1$, the birth targets from time k are considered persistent. Thus, a change of variables is performed such that $\mathbf{X}_{\mathrm{p}} \leftarrow \mathbf{X}_+$ and $\boldsymbol{\pi}_{\mathrm{p}}(\mathbf{X}_{\mathrm{p}}) \leftarrow \boldsymbol{\pi}_+(\mathbf{X}_+)$.

4. DATA-DRIVEN GLMB UPDATE

Measurements are modeled as an RFS consisting of target detections, clutter, and target birth measurements, such that

$$Z = Z_{\mathrm{p}} \cup Z_{\mathrm{b}} \cup Z_{\mathrm{c}}\,, \tag{2}$$

where the "p," "b," and "c" subscripts correspond to persistent targets, birth targets, and clutter, respectively. The false alarm process C is assumed to be Poisson-distributed in time with expected value λ_{c} and distributed in space according to an arbitrary density $\kappa_{\mathrm{c}}(z)/\lambda_{\mathrm{c}}$. The persistent target measurement process $\Upsilon(\mathbf{X}_{\mathrm{p}})$, birth measurement process $B(\mathbf{X}_{\mathrm{b}})$, and false alarm process C are statistically independent.

4.1 Multitarget Likelihood Function

The inclusion of birth target measurements in the multitarget measurement process requires the development of a new multitarget likelihood function. Using FISST, the derivation of this new multitarget likelihood function can be performed in a systematic way. For the sake of exposition, the likelihood function is first developed for the unlabeled RFS, and the labeled equivalent is provided for the final form.

Belief-Mass Function

The multitarget likelihood function is directly related to the belief-mass function, which is defined as $\beta_\Psi(T) \triangleq \Pr(\Psi \subseteq T)$ for some RFS Ψ and closed-set variable T. For the multitarget measurement RFS (Eq. 2), the

belief-mass function is

$$\begin{aligned}\beta_{k+1}(T|X) &= \Pr(\Upsilon(X_\mathrm{p}) \cup C \cup B(X_\mathrm{b}) \subseteq T|X) \\ &= \Pr(\Upsilon(X_\mathrm{p}) \subseteq T,\, C \subseteq T,\, B(X_\mathrm{b}) \subseteq T|X) \\ &= \Pr(\Upsilon(X_\mathrm{p}) \subseteq T|X) \Pr(C \subseteq T) \Pr(B(X_\mathrm{b}) \subseteq T|X) \\ &= \Pr(\Upsilon(X_\mathrm{p}) \subseteq T|X_\mathrm{p}) \Pr(C \subseteq T) \Pr(B(X_\mathrm{b}) \subseteq T|X_\mathrm{b}) \\ &= \beta_{\Upsilon(X_\mathrm{p})}(T) \beta_C(T) \beta_{B(X_\mathrm{b})}(T)\,.\end{aligned}$$

The general product rule for arbitrary set functions $\phi_1(S), \ldots, \phi_n(S)$ is given as[3]

$$\frac{\delta}{\delta Y}(\phi_1(S) \cdots \phi_n(S)) = \sum_{W_1 \uplus \cdots \uplus W_n = Y} \frac{\delta \phi_1}{\delta W_1}(S) \cdots \frac{\delta \phi_n}{\delta W_n}(S)\,,$$

where the summation is taken over all mutually disjoint subsets $W_1, \ldots, W_n$ of Y such that $W_1 \cup \cdots \cup W_n = Y$. Using this rule to take the set derivative of the belief-mass function with respect to Z gives

$$\frac{\delta \beta_{k+1}}{\delta Z}(T|X) = \sum_{Z_\mathrm{p} \uplus Z_\mathrm{b} \uplus Z_\mathrm{c} = Z} \frac{\delta \beta_{\Upsilon(X_\mathrm{p})}}{\delta Z_\mathrm{p}}(T) \cdot \frac{\delta \beta_C}{\delta Z_\mathrm{c}}(T) \cdot \frac{\delta \beta_{B(X_\mathrm{b})}}{\delta Z_\mathrm{b}}(T)\,.$$

To relate the belief-mass function to the probability density, the Radon-Nikodým theorem (Ref. 3, Eq. (11.249)),

$$f_\Psi(Y) = \frac{\delta \beta_\Psi}{\delta Y}(\emptyset)\,,$$

is used. Setting $T = \emptyset$ gives

$$g(Z|X) = \frac{\delta \beta_{k+1}}{\delta Z}(\emptyset|X) = \sum_{Z_\mathrm{p} \uplus Z_\mathrm{b} \uplus Z_\mathrm{c} = Z} f_{\Upsilon(X_\mathrm{p})}(Z_\mathrm{p}) f_C(Z_\mathrm{c}) f_{B(X_\mathrm{b})}(Z_\mathrm{b})\,. \tag{3}$$

Clutter Density

Using the known probability density for Poisson-distributed RFSs, the false alarm probability density is

$$f_C(Z_\mathrm{c}) = e^{-\lambda_\mathrm{c}} \left[\kappa_\mathrm{c}\right]^{Z_\mathrm{c}}\,. \tag{4}$$

Birth Target Measurement Density

Assuming that birth targets are detectable with $p_D = 1$, then $f_{B(X_\mathrm{b})}(Z_\mathrm{b}) = 0$ if $|Z_\mathrm{b}| = e_\mathrm{b} \neq |X_\mathrm{b}|$ and otherwise[3]

$$f_{B(X_\mathrm{b})}(Z_\mathrm{b}) = \sum_\sigma g(z_{\mathrm{b},1}|x_{\mathrm{b},\sigma(1)}) \cdots g(z_{\mathrm{b},n}|x_{\mathrm{b},\sigma(e_\mathrm{b})})\,, \tag{5}$$

where the summation is taken over all permutations σ of the numbers $1, \ldots, e_\mathrm{b}$. Alternatively, for $|Z_\mathrm{b}| = |X_\mathrm{b}|$, define a function $\mu : Z_\mathrm{b} \to X_\mathrm{b}$ by $\mu(z_{\mathrm{b},j}) = x_{\mathrm{b},\sigma(j)}$ such that μ is one-to-one, and any such function $\mu : Z_\mathrm{b} \to X_\mathrm{b}$ defines a permutation σ. With this, Equation (5) can be written as

$$f_{B(X_\mathrm{b})}(Z_\mathrm{b}) = \sum_{\mu\,:\,Z_\mathrm{b} \to X_\mathrm{b}} \left[g(\cdot|\mu(\cdot))\right]^{Z_\mathrm{b}}\,. \tag{6}$$

Persistent Target Measurement Density

In Reference 3, Eq. (12.120), it is shown that if $Z_\mathrm{p} = \{z_{\mathrm{p},1}, \ldots, z_{\mathrm{p},e_\mathrm{p}}\}$ with $|Z_\mathrm{p}| = e_\mathrm{p}$, then $f_{\Upsilon(X_\mathrm{p})} = 0$ if $e_\mathrm{p} > |X_\mathrm{p}|$, and otherwise

$$f_{\Upsilon(X_\mathrm{p})}(Z_\mathrm{p}) = f_{\Upsilon(X_\mathrm{p})}(\emptyset) \sum_{1 \leq i_1 \neq \cdots \neq i_{e_\mathrm{p}} \leq n} \prod_{j=1}^{e_\mathrm{p}} \frac{p_D(x_{i_j}) g(z_{\mathrm{p},j}|x_{i_j})}{1 - p_D(x_{i_j})}\,, \tag{7}$$

where

$$f_{\Upsilon(X_{\mathrm{p}})}(\emptyset) = \left[1 - p_D\right]^{X_{\mathrm{p}}} .$$

Following in the style of Reference 3, Equation (7) can be written more conveniently by defining a function $\tau : Z_{\mathrm{p}} \to X_{\mathrm{p}}$ by $\tau(z_{\mathrm{p},j}) = x_{i_j}$ for all $j = 1, \ldots, e_{\mathrm{p}}$, such that τ is one-to-one, and any such function $\tau : Z_{\mathrm{p}} \to X_{\mathrm{p}}$ defines an e_{p}-tuple $(i_1, \ldots, i_{e_{\mathrm{p}}})$ with $1 \leq i_1 \neq \cdots \neq i_{e_{\mathrm{p}}} \leq n$. With this, Equation (7) is rewritten as

$$f_{\Upsilon(X_{\mathrm{p}})}(Z_{\mathrm{p}}) = f_{\Upsilon(X_{\mathrm{p}})}(\emptyset) \sum_{\tau : Z_{\mathrm{p}} \to X_{\mathrm{p}}} \left[\frac{p_D(\tau(\cdot)) g(\cdot|\tau(\cdot))}{1 - p_D(\tau(\cdot))} \right]^{Z_{\mathrm{p}}} . \tag{8}$$

PROPOSITION 4.1. *Given the clutter density (Eq. 4), birth target measurement density (Eq. 6), and persistent target measurement density (Eq. 8), the multitarget likelihood of the joint measurement set given the joint multitarget state is*

$$\begin{aligned} g(Z|\mathbf{X}) = e^{-\lambda_{\mathrm{c}}} \left[\kappa_{\mathrm{c}}\right]^{Z} \sum_{\theta \in \Theta} \sum_{\vartheta \in \hat{V}} \delta_{\theta^{-1}(\{0:|Z|\})}(\mathcal{L}(\mathbf{X}_{\mathrm{p}})) \delta_{\vartheta^{-1}(\{1:|Z_{\overline{\mathrm{p}}}|\})}(\mathcal{L}(\mathbf{X}_{\mathrm{b}})) \\ \times \frac{|\mathbb{B}|!}{(|\mathbb{B}| - |\mathcal{L}(\mathbf{X}_{\mathrm{b}})|)!} \left[\psi_Z(\cdot;\theta)\right]^{\mathbf{X}_{\mathrm{p}}} \left[\frac{g(z_{\mathrm{b},\vartheta(\ell)}|\cdot)}{\kappa_{\mathrm{c}}(z_{\mathrm{b},\vartheta(\ell)})} \right]^{\mathbf{X}_{\mathrm{b}}} , \end{aligned} \tag{9}$$

where

$$\psi_Z(x, \ell; \theta) = \delta_0(\theta(\ell))(1 - p_D(x, \ell)) + (1 - \delta_0(\theta(\ell))) \frac{p_D(x, \ell) g(z_{\theta(\ell)}|x, \ell)}{\kappa_{\mathrm{c}}(z_{\theta(\ell)})} .$$

Proof: Substituting Equations (4), (6), and (8) into Equation (3) gives

$$\begin{aligned} g(Z|X) &= \sum_{Z_{\mathrm{p}} \uplus Z_{\mathrm{b}} \uplus Z_{\mathrm{c}} = Z} f_{\Upsilon(X_{\mathrm{p}})}(Z_{\mathrm{p}}) f_C(Z_{\mathrm{c}}) f_{B(X_{\mathrm{b}})}(Z_{\mathrm{b}}) \\ &= e^{-\lambda_{\mathrm{c}}} f_{\Upsilon(X_{\mathrm{p}})}(\emptyset) \sum_{Z_{\mathrm{p}} \uplus Z_{\mathrm{b}} \uplus Z_{\mathrm{c}} = Z} \left[\kappa_{\mathrm{c}}\right]^{Z_{\mathrm{c}}} \sum_{\tau : Z_{\mathrm{p}} \to X_{\mathrm{p}}} \left[\frac{p_D(\tau(\cdot)) g(\cdot|\tau(\cdot))}{1 - p_D(\tau(\cdot))} \right]^{Z_{\mathrm{p}}} \sum_{\mu\,:\, Z_{\mathrm{b}} \to X_{\mathrm{b}}} \left[g(\cdot|\mu(\cdot))\right]^{Z_{\mathrm{b}}} . \end{aligned} \tag{10}$$

Using the algebraic relationship

$$f^{Z_{\mathrm{c}}} = \frac{f^Z}{f^{Z - Z_{\mathrm{c}}}} = \frac{f^Z}{f^{Z_{\mathrm{p}}} f^{Z_{\mathrm{b}}}} ,$$

two of the products of Equation (10) can be combined to give

$$g(Z|X) = e^{-\lambda_{\mathrm{c}}} \left[\kappa_{\mathrm{c}}\right]^{Z} f_{\Upsilon(X_{\mathrm{p}})}(\emptyset) \sum_{Z_{\mathrm{p}} \uplus Z_{\mathrm{b}} \uplus Z_{\mathrm{c}} = Z} \sum_{\tau : Z_{\mathrm{p}} \to X_{\mathrm{p}}} \sum_{\mu\,:\, Z_{\mathrm{b}} \to X_{\mathrm{b}}} \left[\frac{p_D(\tau(\cdot)) g(\cdot|\tau(\cdot))}{(1 - p_D(\tau(\cdot)))\kappa_{\mathrm{c}}(\cdot)} \right]^{Z_{\mathrm{p}}} \left[\frac{g(\cdot|\mu(\cdot))}{\kappa_{\mathrm{c}}(\cdot)} \right]^{Z_{\mathrm{b}}} .$$

Let $Z_{\overline{\mathrm{p}}} = Z - Z_{\mathrm{p}} = Z_{\mathrm{c}} \uplus Z_{\mathrm{b}}$, and split the first sum so that

$$g(Z|X) = e^{-\lambda_{\mathrm{c}}} \left[\kappa_{\mathrm{c}}\right]^{Z} f_{\Upsilon(X_{\mathrm{p}})}(\emptyset) \sum_{Z_{\mathrm{p}} \uplus Z_{\overline{\mathrm{p}}} = Z} \sum_{\tau : Z_{\mathrm{p}} \to X_{\mathrm{p}}} \left[\frac{p_D(\tau(\cdot)) g(\cdot|\tau(\cdot))}{(1 - p_D(\tau(\cdot)))\kappa_{\mathrm{c}}(\cdot)} \right]^{Z_{\mathrm{p}}} \sum_{Z_{\mathrm{c}} \uplus Z_{\mathrm{b}} = Z_{\overline{\mathrm{p}}}} \sum_{\mu\,:\, Z_{\mathrm{b}} \to X_{\mathrm{b}}} \left[\frac{g(\cdot|\mu(\cdot))}{\kappa_{\mathrm{c}}(\cdot)} \right]^{Z_{\mathrm{b}}} .$$

Note that, in order to facilitate multiplication with priors of the form of Equation (1), it is desirable to express the product terms over the multitarget state rather than the multitarget measurement. To that end, let $Z \cup \{\phi\}$ be the augmented observation set obtained by appending a dummy variable ϕ, which represents misdetection, to Z. Then, each choice of $Z_{\mathrm{p}} \uplus Z_{\overline{\mathrm{p}}} = Z$ and each choice of one-to-one mapping function $\tau : Z_{\mathrm{p}} \to X_{\mathrm{p}}$ determines a

function $\gamma_{Z_{\mathrm{p},\tau}} : X_{\mathrm{p}} \to Z \cup \{\phi\}$ defined by $\gamma_{Z_{\mathrm{p},\tau}}(x) = z$ if there is a z with $\tau(z) = x$, and $\gamma_{Z_{\mathrm{p},\tau}}(x) = \phi$ otherwise. With this, the first two sums can be combined into one sum over $\gamma_{Z_{\mathrm{p},\tau}}$; that is,

$$g(Z|X) = e^{-\lambda_{\mathrm{c}}} [\kappa_{\mathrm{c}}]^Z f_{\Upsilon(X_{\mathrm{p}})}(\emptyset) \sum_{\gamma\,:\,X_{\mathrm{p}} \to Z \cup \{\phi\}} \left[\frac{p_D(\cdot) g(\gamma(\cdot)|\cdot)}{(1 - p_D(\cdot)) \kappa_{\mathrm{c}}(\gamma(\cdot))} \right]^{\{x\,:\,\gamma(x) \neq \phi\}} \sum_{Z_{\mathrm{c}} \uplus Z_{\mathrm{b}} = Z - \gamma(X_{\mathrm{p}})} \sum_{\mu\,:\,Z_{\mathrm{b}} \to X_{\mathrm{b}}} \left[\frac{g(\cdot|\mu(\cdot))}{\kappa_{\mathrm{c}}(\cdot)} \right]^{Z_{\mathrm{b}}},$$

where $\gamma(x) = \gamma_{Z_{\mathrm{p},\tau}}$ and $\gamma(X_{\mathrm{p}}) = \{\gamma(x_{\mathrm{p},1}), \ldots, \gamma(x_{\mathrm{p},n})\}$ are used for readability.

Furthermore, for each choice of $Z_{\mathrm{c}} \uplus Z_{\mathrm{b}} = Z - \gamma(X_{\mathrm{p}})$ and each choice of function $\mu : Z_{\mathrm{b}} \to X_{\mathrm{b}}$, define the function $\varkappa_{Z_{\mathrm{b}},\mu} : X_{\mathrm{b}} \to Z - \gamma(X_{\mathrm{p}})$ by $\varkappa_{Z_{\mathrm{b}},\mu}(x_{\mathrm{b}}) = z_{\mathrm{b}}$ if there is a z_{b} with $\mu(z_{\mathrm{b}}) = x_{\mathrm{b}}$. Note that because μ is restricted to $|Z_{\mathrm{b}}| = |X_{\mathrm{b}}|$, $\varkappa_{Z_{\mathrm{b}},\mu}$ is undefined over the domain $|X_{\mathrm{b}}| > |Z - \gamma(X_{\mathrm{p}})|$. With this, the last two sums can be combined, and

$$g(Z|X) = e^{-\lambda_{\mathrm{c}}} [\kappa_{\mathrm{c}}]^Z f_{\Upsilon(X_{\mathrm{p}})}(\emptyset) \sum_{\gamma\,:\,X_{\mathrm{p}} \to Z \cup \{\phi\}} \left[\frac{p_D(\cdot) g(\gamma(\cdot)|\cdot)}{(1 - p_D(\cdot)) \kappa_{\mathrm{c}}(\gamma(\cdot))} \right]^{\{x\,:\,\gamma(x) \neq \phi\}} \sum_{\varkappa\,:\,X_{\mathrm{b}} \to Z - \gamma(X_{\mathrm{p}})} \left[\frac{g(\varkappa(\cdot)|\cdot)}{\kappa_{\mathrm{c}}(\varkappa(\cdot))} \right]^{X_{\mathrm{b}}}. \quad (11)$$

Finally, Equation (11) can be expressed in a more tangible form in terms of target-to-measurement associations. Reference 3 defines an association mathematically as a function

$$\theta : \{1, \ldots, |X_{\mathrm{p}}|\} \to \{0, 1, \ldots, |Z|\},$$

where $\theta(i) = 0$ represents a missed detection. For every $i = 1, \ldots, |X_{\mathrm{p}}|$, if $\theta(i) > 0$, then the observation $z_{\theta(i)}$ is uniquely associated with the track x_i, but if $\theta(i) = 0$, then no observation is associated with x_i (the target x_i was not detected). With this, Equation (11) is rewritten as

$$g(Z|X) = e^{-\lambda_{\mathrm{c}}} [\kappa_{\mathrm{c}}]^Z f_{\Upsilon(X_{\mathrm{p}})}(\emptyset) \sum_{\theta} \left[\frac{p_D(x_i) g(z_{\theta(\cdot)}|x_i)}{(1 - p_D(x_i)) \kappa_{\mathrm{c}}(z_{\theta(\cdot)})} \right]^{\{i\,:\,\theta(i) > 0\}} \sum_{\varkappa\,:\,X_{\mathrm{b}} \to Z - Z_\theta} \left[\frac{g(\varkappa(\cdot)|\cdot)}{\kappa_{\mathrm{c}}(\varkappa(\cdot))} \right]^{X_{\mathrm{b}}}, \quad (12)$$

where the first sum is taken over all valid target-to-measurement associations, and $Z_\theta = \{z_{\theta(i)} : \theta(i) > 0\}$. Noting that the set of measurements not assigned to persistent targets $Z_{\overline{\mathrm{p}}} = Z - Z_\theta$, define a birth measurement association function $\vartheta : \{1, \ldots, |X_{\mathrm{b}}|\} \to \{1, \ldots, |Z_{\overline{\mathrm{p}}}|\}$ that has the property $\vartheta(j) = \vartheta(j')$ implies $j = j'$. In other words, a birth target is assigned one and only one measurement. With this, Equation (12) can be written as

$$g(Z|X) = e^{-\lambda_{\mathrm{c}}} [\kappa_{\mathrm{c}}]^Z f_{\Upsilon(X_{\mathrm{p}})}(\emptyset) \sum_{\theta} \left[\frac{p_D(x_i) g(z_{\theta(\cdot)}|x_i)}{(1 - p_D(x_i)) \kappa_{\mathrm{c}}(z_{\theta(\cdot)})} \right]^{\{i\,:\,\theta(i) > 0\}} \sum_{\vartheta} \left[\frac{g(z_{\overline{\mathrm{p}},\vartheta(\cdot)}|x_{\mathrm{b},j})}{\kappa_{\mathrm{c}}(z_{\overline{\mathrm{p}},\vartheta(\cdot)})} \right]^{\{j\,:\,1 \leq j \leq |X_{\mathrm{b}}|\}}. \quad (13)$$

Labeled Equivalent

The labeled equivalent of Equation (13) is

$$\begin{aligned} g(Z|\mathbf{X}) = e^{-\lambda_{\mathrm{c}}} [\kappa_{\mathrm{c}}]^Z f_{\Upsilon(X)}(\emptyset) \sum_{\theta \in \Theta} \sum_{\vartheta \in V} \delta_{\theta^{-1}(\{0:|Z|\})}(\mathcal{L}(\mathbf{X}_{\mathrm{p}})) \delta_{\vartheta^{-1}(\{1:|Z_{\overline{\mathrm{p}}}|\})}(\mathcal{L}(\mathbf{X}_{\mathrm{b}})) \\ \times \left[\frac{p_D(\cdot) g(z_{\theta(\ell)}|\cdot)}{(1 - p_D(\cdot)) \kappa_{\mathrm{c}}(z_{\theta(\ell)})} \right]^{\mathbf{X}_{\mathrm{p}}} \left[\frac{g(z_{\overline{\mathrm{p}},\vartheta(\ell)}|\cdot)}{\kappa_{\mathrm{c}}(z_{\overline{\mathrm{p}},\vartheta(\ell)})} \right]^{\mathbf{X}_{\mathrm{b}}}, \end{aligned} \quad (14)$$

where, as a slight abuse of notation, the new persistent target measurement association map θ is defined over the label space $\mathbb{L}$ rather than over $\{1, \ldots, |\mathbf{X}_{\mathrm{p}}|\}$ and Θ is the space of mappings $\theta : \mathbb{L} \to \{0 : |Z|\}$. Similarly, the birth target measurement association ϑ is defined over the birth label space $\mathbb{B}$ rather than over $\{1, \ldots, |\mathbf{X}_{\mathrm{b}}|\}$, and V is the space of mappings $\vartheta : \mathbb{B} \to \{1 : |Z_{\overline{\mathrm{p}}}|\}$. Note that, while not explicitly denoted, the space V is a function of θ. Also note that a given ϑ need not span the entire birth target label space $\mathbb{B}$; in fact, $\vartheta(\ell \in \mathbb{B})$ undefined implies birth target ℓ does not exist in the given hypothesis. The term $\delta_{\theta^{-1}(\{0:|Z|\})}(\mathcal{L}(\mathbf{X}_{\mathrm{p}}))$, which is equal to 1 when the part of the domain of θ that maps to $\{0 : |Z|\} \triangleq \{0, 1, \ldots, |Z|\}$ matches the labels of $\mathbf{X}_{\mathrm{p}}$,

and 0 otherwise, restricts the summation to valid association maps in Θ. The term $\delta_{\vartheta^{-1}(\{1:|Z_{\overline{\mathrm{p}}}|\})}(\mathcal{L}(\mathbf{X}_{\mathrm{b}}))$, where $\{1:0\} = \emptyset$ by convention, restricts the summation to valid birth target association maps.

In practicality, the full birth target measurement association space V need not be considered, as the inclusion of multiple nearly-identical assignments in which only the birth target label order differs is unnecessary. For example, there is no apparent value in considering two identical birth target initializations, wherein one, the targets are labeled as "1," "2," and "3," and in the other "2," "1," and "4." To address this, define a single unique birth label assignment function $\digamma : \mathbb{B} \to \{1 : |Z|\}$ that obeys the identity: $\digamma(i) = \digamma(i')$ implies that $i = i'$. With this, a reduced birth target measurement association space $\hat{V} \subseteq V$ can be defined as the set of all $\vartheta^{(i)}$ that satisfy $z_{\overline{\mathrm{p}},\vartheta^{(i)}(\ell)} = z_{\digamma(\ell)}$. Using the reduced space $\hat{V}$ ensures that a measurement is associated with at most one unique birth label across *all* hypotheses. Equation (14) can be written in terms of $\hat{V}$ as

$$g(Z|\mathbf{X}) = e^{-\lambda_{\mathrm{c}}} [\kappa_{\mathrm{c}}]^{Z} \sum_{\theta\in\Theta} \sum_{\vartheta\in\hat{V}} \delta_{\theta^{-1}(\{0:|Z|\})}(\mathcal{L}(\mathbf{X}_{\mathrm{p}}))\delta_{\vartheta^{-1}(\{1:|Z_{\overline{\mathrm{p}}}|\})}(\mathcal{L}(\mathbf{X}_{\mathrm{b}}))$$
$$\times \frac{|\mathbb{B}|!}{(|\mathbb{B}| - |\mathcal{L}(\mathbf{X}_{\mathrm{b}})|)!} [\psi_Z(\cdot;\theta)]^{\mathbf{X}_{\mathrm{p}}} \left[\frac{g(z_{\overline{\mathrm{p}},\vartheta(\ell)}|\cdot)}{\kappa_{\mathrm{c}}(z_{\overline{\mathrm{p}},\vartheta(\ell)})}\right]^{\mathbf{X}_{\mathrm{b}}},$$

where

$$\psi_Z(x,\ell;\theta) = \delta_0(\theta(\ell))(1 - p_D(x,\ell)) + (1 - \delta_0(\theta(\ell)))\frac{p_D(x,\ell)g(z_{\theta(\ell)}|x,\ell)}{\kappa_{\mathrm{c}}(z_{\theta(\ell)})}.$$

□

In order to demystify the numerous mapping functions and seemingly complicated measurement indexing, a simple example is presented. The persistent target label space at a given time step is $\mathbb{L} = \{1,2,3\}$. Five measurements are received, and the birth target label space is defined as $\mathbb{B} = \{4,5,6,7,8\}$. This selection ensures that $\mathbb{L} \cap \mathbb{B} = \emptyset$ and allows for the possibility that all five measurements are due to new targets. To ensure that these labels are associated with the same measurements across all hypotheses, the unique birth label assignment function $\digamma : \mathbb{B} \to \{1 : |Z|\}$ is defined as follows: $\digamma(4) = 1$, $\digamma(5) = 2$, $\digamma(6) = 3$, $\digamma(7) = 4$, and $\digamma(8) = 5$. Table 1 shows all of the equivalent measurements using different index functions for a given valid selection of $\theta : \mathbb{L} \to \{0 : |Z|\}$ and ϑ. The persistent target measurement association map shown is given by

Table 1: Measurement equivalence for example target/measurement association maps θ and ϑ.

$\mathbb{B}$	4	5	6	7	8
Z	z_1	z_2	z_3	z_4	z_5
$Z_{\digamma(\mathbb{B})}$	$z_{\digamma(4)}$	$z_{\digamma(5)}$	$z_{\digamma(6)}$	$z_{\digamma(7)}$	$z_{\digamma(8)}$
Z_θ		$z_{\theta(1)}$		$z_{\theta(3)}$	
$Z_{\overline{\mathrm{p}}} = Z - Z_\theta$	$z_{\overline{\mathrm{p}},1}$		$z_{\overline{\mathrm{p}},2}$		$z_{\overline{\mathrm{p}},3}$
Z_{b}	$z_{\mathrm{b},1}$				$z_{\mathrm{b},2}$

$\theta(1) = 2$, $\theta(2) = 0$ (indicating a missed detection for $\ell = 2$), and $\theta(3) = 4$. Given this selection of θ, the birth target association map is defined as $\vartheta(4) = 1$, $\vartheta(8) = 3$, and undefined over the rest of $\mathbb{B}$.

4.2 Bayes Update

The joint posterior density is related to the persistent target prior, birth target prior, and multitarget likelihood function through the Bayes update

$$\boldsymbol{\pi}(\mathbf{X}|Z) = \frac{g(Z|\mathbf{X})\boldsymbol{\pi}_{\mathrm{p}}(\mathbf{X}_{\mathrm{p}})\boldsymbol{\pi}_{\mathrm{b}}(\mathbf{X}_{\mathrm{b}})}{\int g(Z|\mathbf{X})\boldsymbol{\pi}_{\mathrm{p}}(\mathbf{X}_{\mathrm{p}})\boldsymbol{\pi}_{\mathrm{b}}(\mathbf{X}_{\mathrm{b}})\delta\mathbf{X}}.$$

The prior persistent target density is a δ-GLMB distribution of the form

$$\boldsymbol{\pi}_{\mathrm{p}}(\mathbf{X}_{\mathrm{p}}) = \Delta(\mathbf{X}_{\mathrm{p}}) \sum_{\xi\in\Xi} w^{(\xi)}(\mathcal{L}(\mathbf{X}_{\mathrm{p}}))[p^{(\xi)}]^{\mathbf{X}_{\mathrm{p}}}, \tag{15}$$

where $\Delta(\mathbf{X}_\mathrm{p})$ is the distinct label indicator $\delta_{(|\mathbf{X}_\mathrm{p}|)}(|\mathcal{L}(\mathbf{X}_\mathrm{p})|)$. The prior birth target density is assumed to be Poisson, given by

$$\boldsymbol{\pi}_\mathrm{b}(\mathbf{X}_\mathrm{b}) = \Delta(\mathbf{X}_\mathrm{b}) w_\mathrm{b}(\mathcal{L}(\mathbf{X}_\mathrm{b}))[p_\mathrm{b}]^{\mathbf{X}_\mathrm{b}}\,, \tag{16}$$

where

$$\begin{aligned} p_\mathrm{b}(x,\ell) &= v_\mathrm{b}(x)/\left\langle v_\mathrm{b}, 1\right\rangle\,, \\ w_\mathrm{b}(B) &= 1_{\mathbb{B}}(B)\mathrm{Pois}_{\langle v_\mathrm{b},1\rangle}(|B|)\frac{(|\mathbb{B}|-|B|)!}{|\mathbb{B}|!}\,, \\ \mathrm{Pois}_\lambda(n) &\triangleq e^{-\lambda}\lambda^n/n!\,, \end{aligned}$$

and $v_\mathrm{b}(x)$ is the PHD of birth targets. The Poisson density is a natural choice for modeling target birth when little information is known *a priori*. In operational tracking, specification of every possible birth target's probability of existence is non-intuitive if no other information is available. A "best guess" of the rate that new targets appear is typically less restrictive and is sufficient to fully describe the Poisson cardinality distribution. Intuitively, the use of a Poisson density changes the question from "What is the likelihood that new targets 2 and 3 are born?" to "What is the likelihood that two targets are born?"

PROPOSITION 4.2. *Given the persistent multitarget prior (Eq. 15), birth multitarget prior (Eq. 16), and likelihood function (Eq. 9), the joint multitarget posterior density is given by*

$$\boldsymbol{\pi}(\mathbf{X}|Z) = \Delta(\mathbf{X}_\mathrm{p})\Delta(\mathbf{X}_\mathrm{b}) \sum_{\xi\in\Xi}\sum_{\theta\in\Theta}\sum_{\vartheta\in\hat{V}} w_Z^{(\xi,\theta,\vartheta)}(\mathcal{L}(\mathbf{X}))[p^{(\xi,\theta,\vartheta)}(\cdot|Z)]^{\mathbf{X}}\,,$$

where

$$w_Z^{(\xi,\theta,\vartheta)}(L) \triangleq \frac{\delta_{\theta^{-1}(\{0:|Z|\})}(L\cap\mathbb{L})\delta_{\vartheta^{-1}(\{1:|Z_{\overline{\mathrm{p}}}|\})}(L-\mathbb{L})w^{(\xi)}(L\cap\mathbb{L})\tilde{w}_\mathrm{b}(L-\mathbb{L})[\eta_Z^{(\xi,\theta)}]^{L\cap\mathbb{L}}\left[\frac{p_\mathrm{b}(z_{\overline{\mathrm{p}},\vartheta(\cdot)})}{\kappa_\mathrm{c}(z_{\overline{\mathrm{p}},\vartheta(\ell)})}\right]^{L-\mathbb{L}}}{\sum_{\xi\in\Xi}\sum_{\theta\in\Theta}\sum_{\vartheta\in\hat{V}}\sum_{J\in\mathcal{F}(\mathbb{L})}\sum_{B\in\mathcal{F}(\mathbb{B})}\delta_{\theta^{-1}(\{0:|Z|\})}(J)\delta_{\vartheta^{-1}(\{1:|Z_{\overline{\mathrm{p}}}|\})}(B)\tilde{w}_\mathrm{b}(B)w^{(\xi)}(J)\left[\eta_Z^{(\xi,\theta)}\right]^J\left[\frac{p_\mathrm{b}(z_{\overline{\mathrm{p}},\vartheta(\cdot)})}{\kappa_\mathrm{c}(z_{\overline{\mathrm{p}},\vartheta(\cdot)})}\right]^B}\,,$$

and

$$\begin{aligned} p^{(\xi,\theta,\vartheta)}(x,\ell|Z) &\triangleq 1_{\mathbb{L}}(\ell)p^{(\xi,\theta)}(x,\ell|Z) + (1-1_{\mathbb{L}}(\ell))p_\mathrm{b}^{(\vartheta)}(x,\ell|Z)\,, \\ p^{(\xi,\theta)}(x,\ell|Z) &\triangleq \frac{p^{(\xi)}(x,\ell)\psi_Z(x,\ell;\theta)}{\eta_Z^{(\xi,\theta)}(\ell)}\,, \qquad (17) \\ \eta_Z^{(\xi,\theta)}(\ell) &= \left\langle p^{(\xi)}(\cdot,\ell), \psi_Z(\cdot,\ell;\theta)\right\rangle, \\ p_\mathrm{b}^{(\vartheta)}(x,\ell|Z) &\triangleq \frac{g(z_{\overline{\mathrm{p}},\vartheta(\ell)}|x)p_\mathrm{b}(x)}{\left\langle g(z_{\overline{\mathrm{p}},\vartheta(\ell)}|\cdot),\, p_\mathrm{b}(\cdot)\right\rangle}\,, \qquad (18) \\ p_\mathrm{b}(z) &\triangleq \left\langle g(z|\cdot),\, p_\mathrm{b}(\cdot)\right\rangle\,. \end{aligned}$$

Proof: Multiplication of the multitarget priors (Eqs. 15 and 16) and the likelihood function (Eq. 9) gives

$$\begin{aligned} g(Z|\mathbf{X})\boldsymbol{\pi}_\mathrm{p}(\mathbf{X}_\mathrm{p})\boldsymbol{\pi}_\mathrm{b}(\mathbf{X}_\mathrm{b}) = \Delta(\mathbf{X}_\mathrm{p})\Delta(\mathbf{X}_\mathrm{b})e^{-\lambda_\mathrm{c}}\kappa_\mathrm{c}^Z \sum_{\xi\in\Xi}\sum_{\theta\in\Theta}\sum_{\vartheta\in\hat{V}}\delta_{\theta^{-1}(\{0:|Z|\})}(\mathcal{L}(\mathbf{X}_\mathrm{p}))\delta_{\vartheta^{-1}(\{1:|Z_{\overline{\mathrm{p}}}|\})}(\mathcal{L}(\mathbf{X}_\mathrm{b})) \\ \times w^{(\xi)}(\mathcal{L}(\mathbf{X}_\mathrm{p}))\tilde{w}_\mathrm{b}(\mathcal{L}(\mathbf{X}_\mathrm{b}))[p^{(\xi)}(\cdot)\psi_Z(\cdot,\theta)]^{\mathbf{X}_\mathrm{p}}\left[\frac{g(z_{\overline{\mathrm{p}},\vartheta(\ell)}|\cdot)p_\mathrm{b}(\cdot)}{\kappa_\mathrm{c}(z_{\overline{\mathrm{p}},\vartheta(\ell)})}\right]^{\mathbf{X}_\mathrm{b}}\,, \end{aligned}$$

where

$$\tilde{w}_\mathrm{b}(B) \triangleq w_\mathrm{b}(B)\frac{|\mathbb{B}|!}{(|\mathbb{B}|-|B|)!} = 1_{\mathbb{B}}(B)\mathrm{Pois}_{\langle v_\mathrm{b},1\rangle}(|B|)\,.$$

Substituting Equation (17) gives

$$g(Z|\mathbf{X})\boldsymbol{\pi}_{\mathrm{p}}(\mathbf{X}_{\mathrm{p}})\boldsymbol{\pi}_{\mathrm{b}}(\mathbf{X}_{\mathrm{b}}) = \Delta(\mathbf{X}_{\mathrm{p}})\Delta(\mathbf{X}_{\mathrm{b}})e^{-\lambda_{\mathrm{c}}}\kappa_{\mathrm{c}}^{Z}\sum_{\xi\in\Xi}\sum_{\theta\in\Theta}\sum_{\vartheta\in\hat{V}}\delta_{\theta^{-1}(\{0:|Z|\})}(\mathcal{L}(\mathbf{X}_{\mathrm{p}}))\delta_{\vartheta^{-1}(\{1:|Z_{\overline{\mathrm{p}}}|\})}(\mathcal{L}(\mathbf{X}_{\mathrm{b}}))$$
$$\times w^{(\xi)}(\mathcal{L}(\mathbf{X}_{\mathrm{p}}))\tilde{w}_{\mathrm{b}}(\mathcal{L}(\mathbf{X}_{\mathrm{b}}))[\eta_{Z}^{(\xi,\theta)}]^{\mathcal{L}(\mathbf{X}_{\mathrm{p}})}[p^{(\xi,\theta)}(\cdot|Z)]^{\mathbf{X}_{\mathrm{p}}}\left[\frac{g(z_{\overline{\mathrm{p}},\vartheta(\ell)}|\cdot)p_{\mathrm{b}}(\cdot)}{\kappa_{\mathrm{c}}(z_{\overline{\mathrm{p}},\vartheta(\ell)})}\right]^{\mathbf{X}_{\mathrm{b}}}. \quad (19)$$

Now, consider the integral

$$\int g(Z|\mathbf{X})\boldsymbol{\pi}_{\mathrm{p}}(\mathbf{X}_{\mathrm{p}})\boldsymbol{\pi}_{\mathrm{b}}(\mathbf{X}_{\mathrm{b}})\delta\mathbf{X}$$
$$= e^{-\lambda_{\mathrm{c}}}\kappa_{\mathrm{c}}^{Z}\int\Delta(\mathbf{X}_{\mathrm{p}})\Delta(\mathbf{X}_{\mathrm{b}})\sum_{\xi\in\Xi}\sum_{\theta\in\Theta}\sum_{\vartheta\in\hat{V}}\delta_{\theta^{-1}(\{0:|Z|\})}(\mathcal{L}(\mathbf{X}_{\mathrm{p}}))\delta_{\vartheta^{-1}(\{1:|Z_{\overline{\mathrm{p}}}|\})}(\mathcal{L}(\mathbf{X}_{\mathrm{b}}))$$
$$\times w^{(\xi)}(\mathcal{L}(\mathbf{X}_{\mathrm{p}}))\tilde{w}_{\mathrm{b}}(\mathcal{L}(\mathbf{X}_{\mathrm{b}}))[\eta_{Z}^{(\xi,\theta)}]^{\mathcal{L}(\mathbf{X}_{\mathrm{p}})}[p^{(\xi,\theta)}(\cdot|Z)]^{\mathbf{X}_{\mathrm{p}}}\left[\frac{g(z_{\overline{\mathrm{p}},\vartheta(\ell)}|\cdot)p_{\mathrm{b}}(\cdot)}{\kappa_{\mathrm{c}}(z_{\overline{\mathrm{p}},\vartheta(\ell)})}\right]^{\mathbf{X}_{\mathrm{b}}}\delta\mathbf{X}$$

$$= e^{-\lambda_{\mathrm{c}}}\kappa_{\mathrm{c}}^{Z}\sum_{\xi\in\Xi}\sum_{\theta\in\Theta}\sum_{\vartheta\in\hat{V}}\int\Delta(\mathbf{X}_{\mathrm{p}})\delta_{\theta^{-1}(\{0:|Z|\})}(\mathcal{L}(\mathbf{X}_{\mathrm{p}}))w^{(\xi)}(\mathcal{L}(\mathbf{X}_{\mathrm{p}}))[\eta_{Z}^{(\xi,\theta)}]^{\mathcal{L}(\mathbf{X}_{\mathrm{p}})}[p^{(\xi,\theta)}(\cdot|Z)]^{\mathbf{X}_{\mathrm{p}}}\delta\mathbf{X}_{\mathrm{p}}$$
$$\times\int\Delta(\mathbf{X}_{\mathrm{b}})\delta_{\vartheta^{-1}(\{1:|Z_{\overline{\mathrm{p}}}|\})}(\mathcal{L}(\mathbf{X}_{\mathrm{b}}))\tilde{w}_{\mathrm{b}}(\mathcal{L}(\mathbf{X}_{\mathrm{b}}))\left[\frac{g(z_{\overline{\mathrm{p}},\vartheta(\ell)}|\cdot)p_{\mathrm{b}}(\cdot)}{\kappa_{\mathrm{c}}(z_{\overline{\mathrm{p}},\vartheta(\ell)})}\right]^{\mathbf{X}_{\mathrm{b}}}\delta\mathbf{X}_{\mathrm{b}}\,. \quad (20)$$

Lemma 3 of Reference 12 states

> Let $\Delta(\mathbf{X})$ denote the distinct label indicator $\delta_{|\mathbf{X}|}(|\mathcal{L}(\mathbf{X})|)$. Then for $h : \mathcal{F}(\mathbb{L}) \to \mathbb{R}$ and $g : \mathbb{X}\times\mathbb{L}\to\mathbb{R}$, integrable on $\mathbb{X}$,
>
> $$\int\Delta(\mathbf{X})h(\mathcal{L}(\mathbf{X}))g^{\mathbf{X}}\delta\mathbf{X} = \sum_{L\in\mathcal{F}(\mathbb{L})}h(L)\left[\int g(x,\cdot)\mathrm{d}x\right]^{L}.$$

Applying this lemma to the integral over $\mathbf{X}_{\mathrm{p}}$ and the integral over $\mathbf{X}_{\mathrm{b}}$ in Equation (20) gives

$$\int g(Z|\mathbf{X})\boldsymbol{\pi}_{\mathrm{p}}(\mathbf{X}_{\mathrm{p}})\boldsymbol{\pi}_{\mathrm{b}}(\mathbf{X}_{\mathrm{b}})\delta\mathbf{X} = e^{-\lambda_{\mathrm{c}}}\kappa_{\mathrm{c}}^{Z}\sum_{\xi\in\Xi}\sum_{\theta\in\Theta}\sum_{\vartheta\in\hat{V}}\sum_{J\in\mathcal{F}(\mathbb{L})}\sum_{B\in\mathcal{F}(\mathbb{B})}\delta_{\theta^{-1}(\{0:|Z|\})}(J)\delta_{\vartheta^{-1}(\{1:|Z_{\overline{\mathrm{p}}}|\})}(B)$$
$$\times\tilde{w}_{\mathrm{b}}(B)w^{(\xi)}(J)\left[\eta_{Z}^{(\xi,\theta)}\right]^{J}\left[\int\frac{g(z_{\overline{\mathrm{p}},\vartheta(\cdot)}|x,\cdot)p_{\mathrm{b}}(x,\cdot)}{\kappa_{\mathrm{c}}(z_{\overline{\mathrm{p}},\vartheta(\cdot)})}\mathrm{d}x\right]^{B}.$$

Define the marginal birth density over the measurement space as

$$p_{\mathrm{b}}(z,\ell) \triangleq \langle g(z|\cdot,\ell),\, p_{\mathrm{b}}(\cdot,\ell)\rangle\,. \quad (21)$$

If the individual birth measurement likelihood is independent of target label ($g(z_{\overline{\mathrm{p}},\vartheta(\cdot)}|x,\ell) = g(z_{\overline{\mathrm{p}},\vartheta(\cdot)}|x)$) and the individual target birth density is independent of target label ($p_{\mathrm{b}}(x,\ell) = p_{\mathrm{b}}(x)$, which is true under the Poisson birth assumption), then $p_{\mathrm{b}}(z,\ell) = p_{\mathrm{b}}(z)$. With this,

$$\int g(Z|\mathbf{X})\boldsymbol{\pi}_{\mathrm{p}}(\mathbf{X}_{\mathrm{p}})\boldsymbol{\pi}_{\mathrm{b}}(\mathbf{X}_{\mathrm{b}})\delta\mathbf{X} = e^{-\lambda_{\mathrm{c}}}\kappa_{\mathrm{c}}^{Z}\sum_{\xi\in\Xi}\sum_{\theta\in\Theta}\sum_{\vartheta\in\hat{V}}\sum_{J\in\mathcal{F}(\mathbb{L})}\sum_{B\in\mathcal{F}(\mathbb{B})}\delta_{\theta^{-1}(\{0:|Z|\})}(J)\delta_{\vartheta^{-1}(\{1:|Z_{\overline{\mathrm{p}}}|\})}(B)$$
$$\times\tilde{w}_{\mathrm{b}}(B)w^{(\xi)}(J)\left[\eta_{Z}^{(\xi,\theta)}\right]^{J}\left[\frac{p_{\mathrm{b}}(z_{\overline{\mathrm{p}},\vartheta(\cdot)})}{\kappa_{\mathrm{c}}(z_{\overline{\mathrm{p}},\vartheta(\cdot)})}\right]^{B}. \quad (22)$$

Going back to the Bayes update numerator term (Eq. 19) and substituting Equation (21),

$$g(Z|\mathbf{X})\boldsymbol{\pi}_{\mathrm{p}}(\mathbf{X}_{\mathrm{p}})\boldsymbol{\pi}_{\mathrm{b}}(\mathbf{X}_{\mathrm{b}}) = \Delta(\mathbf{X}_{\mathrm{p}})\Delta(\mathbf{X}_{\mathrm{b}})e^{-\lambda_{\mathrm{c}}}\kappa_{\mathrm{c}}^{Z}\sum_{\xi\in\Xi}\sum_{\theta\in\Theta}\sum_{\vartheta\in\hat{V}}\delta_{\theta^{-1}(\{0:|Z|\})}(\mathcal{L}(\mathbf{X}_{\mathrm{p}}))\delta_{\vartheta^{-1}(\{1:|Z_{\overline{\mathrm{p}}}|\})}(\mathcal{L}(\mathbf{X}_{\mathrm{b}}))$$
$$\times\, w^{(\xi)}(\mathcal{L}(\mathbf{X}_{\mathrm{p}}))\tilde{w}_{\mathrm{b}}(\mathcal{L}(\mathbf{X}_{\mathrm{b}}))[\eta_{Z}^{(\xi,\theta)}]^{\mathcal{L}(\mathbf{X}_{\mathrm{p}})}[p^{(\xi,\theta)}(\cdot|Z)]^{\mathbf{X}_{\mathrm{p}}}\left[\frac{p_{\mathrm{b}}(z_{\overline{\mathrm{p}},\vartheta(\cdot)})p_{\mathrm{b}}^{(\vartheta)}(\cdot|Z)}{\kappa_{\mathrm{c}}(z_{\overline{\mathrm{p}},\vartheta(\ell)})}\right]^{\mathbf{X}_{\mathrm{b}}}. \quad (23)$$

Finally, using Equations (22) and (23) and applying Bayes' rule, the posterior multitarget density is obtained as

$$\boldsymbol{\pi}(\mathbf{X}|Z) = \frac{g(Z|\mathbf{X})\boldsymbol{\pi}_{\mathrm{p}}(\mathbf{X}_{\mathrm{p}})\boldsymbol{\pi}_{\mathrm{b}}(\mathbf{X}_{\mathrm{b}})}{\int g(Z|\mathbf{X})\boldsymbol{\pi}_{\mathrm{p}}(\mathbf{X}_{\mathrm{p}})\boldsymbol{\pi}_{\mathrm{b}}(\mathbf{X}_{\mathrm{b}})\delta\mathbf{X}}$$
$$= \Delta(\mathbf{X}_{\mathrm{p}})\Delta(\mathbf{X}_{\mathrm{b}})\sum_{\xi\in\Xi}\sum_{\theta\in\Theta}\sum_{\vartheta\in\hat{V}}w_{Z}^{(\xi,\theta,\vartheta)}(\mathcal{L}(\mathbf{X}))[p^{(\xi,\theta,\vartheta)}(\cdot|Z)]^{\mathbf{X}}.$$

□

4.3 Special Case: Linear-Gaussian Measurements, Uniform Birth Spatial Density

If the single-target measurement likelihood function is linear-Gaussian, such that

$$g(z|x,\ell) = g(z|x) = \mathcal{N}(z; Hx, R),$$

and the birth target spatial density $p_{\mathrm{b}}(x,\ell) = p_{\mathrm{b}}(x) = \mathcal{U}_{\mathbb{X}}(x) \triangleq 1/V_{\mathbb{X}}$, then the measurement-marginal target birth density (Eq. 21) is

$$p_{\mathrm{b}}(z) \approx \mathcal{U}_{\mathbb{Z}}(z) \triangleq 1/V_{\mathbb{Z}}$$

for sufficiently small R, where $V_{\mathbb{X}}$ and $V_{\mathbb{Z}}$ are the "scene volumes" in the single-target kinematic space and single-target measurement space, respectively.

Furthermore, if the entire single-target state space is measurable and the observation function is one-to-one, Equation (18) can be approximated by

$$p_{\mathrm{b}}^{(\vartheta)}(x,\ell|Z) = \mathcal{N}(x; H^{-1}z_{\overline{\mathrm{p}},\vartheta(\ell)},\, H^{-1}RH^{-T}).$$

In many linear tracking problems, only part of the state is directly observed by a single measurement. Denote the observed portion of that state by $\tilde{x}$ and the non-observed portion by $\overline{x}$ such that $x^T = [\tilde{x}^T, \overline{x}^T]$. Denote by $\tilde{H}$ the nonsingular reduced observation matrix, such that $g(z|x) = g(z|\tilde{x}) = \mathcal{N}(z; \tilde{H}\tilde{x}, R)$. The density $p_{\mathrm{b}}(\overline{x},\ell)$ of the unobservable portion of the state is the marginal $\int p_{\mathrm{b}}(x,\ell)\mathrm{d}\tilde{x}$. The measurement-conditioned single-target birth density is then

$$p_{\mathrm{b}}^{(\vartheta)}(x,\ell|Z) = \left[\begin{array}{c}\mathcal{N}(\tilde{x}; \tilde{H}^{-1}z_{\overline{\mathrm{p}},\vartheta(\ell)},\, \tilde{H}^{-1}R\tilde{H}^{-T}) \\ p_{\mathrm{b}}(\overline{x},\ell)\end{array}\right].$$

5. PREDICTION

In the prediction stage, the posterior density undergoes a time-update to produce the density at time $k+1$, which is denoted by $\boldsymbol{\pi}_{+}(\mathbf{X}_{+})$. The posterior density is propagated forward in time according to the multitarget Chapman-Kolmogorov equation

$$\boldsymbol{\pi}_{+}(\mathbf{X}_{+}) = \int \mathbf{f}(\mathbf{X}_{+}|\mathbf{X})\boldsymbol{\pi}(\mathbf{X})\delta\mathbf{X}. \quad (24)$$

The transition density $\mathbf{f}(\mathbf{X}_{+}|\mathbf{X})$ describes both target survival and kinematic state evolution. Each target either survives with probability $p_S(x,\ell)$ or dies with probability $q_S(x,\ell) = 1 - p_S(x,\ell)$. A surviving target state evolves

probabilistically to a new state (x_+, ℓ_+) according to the single-target transition density $f(x_+|x,\ell)\delta_\ell(\ell_+)$. From Reference 12, the multitarget transition density can be written in GLMB form as

$$\mathbf{f}(\mathbf{X}_+|\mathbf{X}) = \Delta(\mathbf{X}_+)\Delta(\mathbf{X})1_{\mathcal{L}(\mathbf{X})}(\mathcal{L}(\mathbf{X}_+))[\Phi(\mathbf{X}_+;\cdot)]^{\mathbf{X}}\,, \tag{25}$$

where

$$\Phi(\mathbf{X}_+;x,\ell) \triangleq \sum_{(x_+,\ell_+)\in\mathbf{X}_+} \delta_\ell(\ell_+)p_S(x,\ell)f(x_+|x,\ell) + [1-1_{\mathcal{L}(\mathbf{X}_+)}(\ell)]q_S(x,\ell)\,.$$

In Equation (25), the term $1_{\mathcal{L}(\mathbf{X})}(\mathcal{L}(\mathbf{X}_+))$ ensures that the new multitarget label set contains no labels not present in $\mathcal{L}(\mathbf{X})$.

PROPOSITION 5.1. *Given a posterior GLMB density of the form of Equation (1) and multitarget transition density given by Equation (25), the predicted density is also a GLMB density given by*

$$\boldsymbol{\pi}_+(\mathbf{X}_+) = \Delta(\mathbf{X}_+)\sum_{\xi\in\Xi} w_S^{(\xi)}(\mathcal{L}(\mathbf{X}_+))[p_S^{(\xi)}]^{\mathbf{X}_+}\,,$$

where

$$\begin{aligned}
w_S^{(\xi)}(I) &\triangleq [\eta_S^{(\xi)}]^I \sum_{J\in\mathcal{F}(\mathbb{L})} 1_J(I)[q_S^{(\xi)}]^{J-I}w^{(\xi)}(J)\,,\\
\eta_S^{(\xi)}(\ell) &\triangleq \int \left\langle p_S(\cdot,\ell)f(x|\cdot,\ell), p^{(\xi)}(\cdot,\ell)\right\rangle \mathrm{d}x\,,\\
q_s^{(\xi)} &\triangleq \left\langle q_S(\cdot,\ell),\, p^{(\xi)}(\cdot,\ell)\right\rangle\,, \qquad \textit{and}\\
p_S^{(\xi)}(x,\ell) &\triangleq \frac{\left\langle p_S(\cdot,\ell)f(x|\cdot,\ell),\, p^{(\xi)}(\cdot,\ell)\right\rangle}{\eta_S^{(\xi)}(\ell)}\,.
\end{aligned}$$

Proof: Substituting Equation (25) into Equation (24),

$$\begin{aligned}
\boldsymbol{\pi}_+(\mathbf{X}_+) &= \Delta(\mathbf{X}_+)\sum_{\xi\in\Xi}\int \Delta(\mathbf{X})\,1_{\mathcal{L}(\mathbf{X})}(\mathcal{L}(\mathbf{X}_+))w^{(\xi)}(\mathcal{L}(\mathbf{X}))[\Phi(\mathbf{X}_+;\cdot)p^{(\xi)}]^{\mathbf{X}}\delta\mathbf{X}\\
&= \Delta(\mathbf{X}_+)\sum_{\xi\in\Xi}\sum_{I\in\mathcal{F}(\mathbb{L})} 1_I(\mathcal{L}(\mathbf{X}_+))w^{(\xi)}(I)\prod_{\ell\in I}\left\langle \Phi(\mathbf{X}_+;\cdot,\ell),\, p^{(\xi)}(\cdot,\ell)\right\rangle\,.
\end{aligned} \tag{26}$$

The product in Equation (26) can be separated into two products over persistent target labels and non-surviving (death) target labels as

$$\begin{aligned}
&\prod_{\ell\in I}\left\langle \Phi(\mathbf{X}_+;\cdot,\ell),\, p^{(\xi)}(\cdot,\ell)\right\rangle\\
&\quad= \prod_{\ell\in\mathcal{L}(\mathbf{X}_+)}\left\langle \Phi(\mathbf{X}_+;\cdot,\ell),\, p^{(\xi)}(\cdot,\ell)\right\rangle \prod_{\ell\in I-\mathcal{L}(\mathbf{X}_+)}\left\langle \Phi(\mathbf{X}_+;\cdot,\ell),\, p^{(\xi)}(\cdot,\ell)\right\rangle\\
&\quad= \prod_{\ell\in\mathcal{L}(\mathbf{X}_+)}\sum_{(x_+,\ell_+)\in\mathbf{X}_+}\delta_\ell(\ell_+)\left\langle p_S(\cdot,\ell)f(x_+|\cdot,\ell),\, p^{(\xi)}(\cdot,\ell)\right\rangle \prod_{\ell\in I-\mathcal{L}(\mathbf{X}_+)}\left\langle q_S(\cdot,\ell), p^{(\xi)}(\cdot,\ell)\right\rangle\\
&\quad= \prod_{\ell\in\mathcal{L}(\mathbf{X}_+)}\sum_{(x_+,\ell_+)\in\mathbf{X}_+}\delta_\ell(\ell_+)p_S^{(\xi)}(x_+,\ell)\eta_S^{(\xi)}(\ell) \prod_{\ell\in I-\mathcal{L}(\mathbf{X}_+)} q_S^{(\xi)}(\ell)\,,
\end{aligned} \tag{27}$$

Because the sum in Equation (27) has only one nonzero term (when $\ell = \ell_+$), it can be combined with the product so that

$$\begin{aligned}\prod_{\ell\in I}\left\langle \Phi(\mathbf{X}_+;\cdot,\ell),\, p^{(\xi)}(\cdot,\ell)\right\rangle &= \prod_{(x_+,\ell_+)\in\mathbf{X}_+} p_S^{(\xi)}(x_+,\ell)\eta_S^{(\xi)}(\ell) \prod_{\ell\in I-\mathcal{L}(\mathbf{X}_+)} q_S^{(\xi)}(\ell) \\ &= [p_S^{(\xi)}]^{\mathbf{X}_+}[\eta_S^{(\xi)}]^{\mathcal{L}(\mathbf{X}_+)}[q_S^{(\xi)}]^{I-\mathcal{L}(\mathbf{X}_+)}\,.\end{aligned}$$

This simplified expression can be substituted into Equation (26) to produce the final time-update equation as

$$\begin{aligned}\boldsymbol{\pi}_+(\mathbf{X}_+) &= \Delta(\mathbf{X}_+)\sum_{\xi\in\Xi}\sum_{I\in\mathcal{F}(\mathbb{L})} 1_I(\mathcal{L}(\mathbf{X}_+))w^{(\xi)}(I)[p_S^{(\xi)}]^{\mathbf{X}_+}[\eta_S^{(\xi)}]^{\mathcal{L}(\mathbf{X}_+)}[q_S^{(\xi)}]^{I-\mathcal{L}(\mathbf{X}_+)} \\ &= \Delta(\mathbf{X}_+)\sum_{\xi\in\Xi} w_S^{(\xi)}(\mathcal{L}(\mathbf{X}_+))[p_S^{(\xi)}]^{\mathbf{X}_+}\,.\end{aligned}$$

□

6. δ-GENERALIZATION

For more straightforward implementation, the data-driven GLMB can be written in δ-generalized form, which simply makes use of the identity

$$w^{(\xi)}(J) = \sum_{I\in\mathcal{F}(\mathbb{L})} w^{(\xi)}(I)\delta_I(J)\,.$$

With this, a standard GLMB distribution can be written as a δ-GLMB as

$$\boldsymbol{\pi}(\mathbf{X}) = \Delta(\mathbf{X})\sum_{(I,\xi)\in\mathcal{F}(\mathbb{L})\times\Xi}\omega^{(I,\xi)}\delta_I(\mathcal{L}(\mathbf{X}))[p^{(\xi)}]^{\mathbf{X}}\,,$$

where $\omega^{(I,\xi)} \triangleq w^{(\xi)}(I)$.

6.1 Data-Driven δ-GLMB Update

Given a prior δ-GLMB of the form

$$\boldsymbol{\pi}(\mathbf{X}) = \Delta(\mathbf{X})\sum_{(I,\xi)\in\mathcal{F}(\mathbb{L})\times\Xi}\omega^{(I,\xi)}\delta_I(\mathcal{L}(\mathbf{X}))[p^{(\xi)}]^{\mathbf{X}}\,,$$

the measurement-updated posterior is

$$\boldsymbol{\pi}(\mathbf{X}|Z) = \Delta(\mathbf{X})\sum_{(I,\xi)\in\mathcal{F}(\mathbb{L})\times\Xi}\sum_{\theta\in\Theta}\sum_{\vartheta\in\hat{V}}\omega^{(I,\xi,\theta,\vartheta)}(Z)\delta_I(\mathcal{L}(\mathbf{X}))\left[p^{(\xi,\theta,\vartheta)}(\cdot|Z)\right]^{\mathbf{X}}\,,$$

where $\omega^{(I,\xi,\theta,\vartheta)}(Z) \triangleq w_Z^{(\xi,\theta,\vartheta)}(I)$.

6.2 Data-Driven δ-GLMB Prediction

Given a posterior δ-GLMB density of the form

$$\boldsymbol{\pi}(\mathbf{X}) = \Delta(\mathbf{X})\sum_{(I,\xi)\in\mathcal{F}(\mathbb{L})\times\Xi}\omega^{(I,\xi)}\delta_I(\mathcal{L}(\mathbf{X}))[p^{(\xi)}]^{\mathbf{X}}\,,$$

the time-updated prior is

$$\boldsymbol{\pi}_+(\mathbf{X}_+) = \Delta(\mathbf{X}_+)\sum_{(I,\xi)\in\mathcal{F}(\mathbb{L})\times\Xi}\omega_S^{(I,\xi)}\delta_I(\mathcal{L}(\mathbf{X}_+))[p_S^{(\xi)}]^{\mathbf{X}_+}\,,$$

where $\omega_S^{(I,\xi)} \triangleq w_S^{(\xi)}(I)$.

7. NUMERICAL EXAMPLE

7.1 Example 1

To evaluate the performance of the data-driven δ-GLMB filter, a simulation is performed with numerous target births. The single-target state $x_k = [r_{x,k}, r_{y,k}, \dot{r}_{x,k}, \dot{r}_{y,k}]^T$ consists of the Cartesian position and velocity of the target. The true number of births at every time step is sampled from a Poisson distribution with mean $\lambda_{\text{b}} = 2.0$. The birth targets' true initial positional states are sampled uniformly over the scene, and the true initial velocities are sampled from a zero-mean Gaussian distribution with standard deviation $\sigma_{\dot{r}} = 0.05\,[\text{m/s}]$. The simulation begins with three true targets and concludes with 28, with 30 true targets in total (two target deaths). The true paths of all thirty targets are shown in Figure 3.

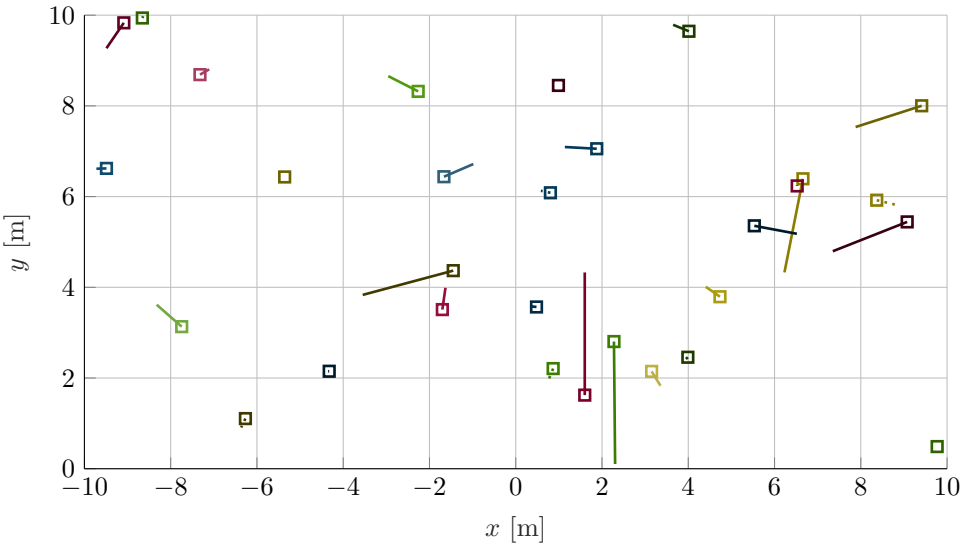

Figure 3: Simulated true motion. Starting locations are represented by square markers.

Target motion is propagated via a constant-velocity model given as

$$x_{k+1} = F_k x_k + M_k \eta_k \,,$$

where η_k is a 2×1 Gaussian white noise vector with $E\{\eta_k \eta_k^T\} = Q_k$,

$$F_k = \begin{bmatrix} 1 & 0 & \Delta t & 0. \\ 0 & 1 & 0 & \Delta t \\ 0 & 0 & 1 & 0 \\ 0 & 0 & 0 & 1 \end{bmatrix}, \quad \text{and} \quad M_k = \begin{bmatrix} 0 & 0 \\ 0 & 0 \\ \sqrt{\Delta t} & 0 \\ 0 & \sqrt{\Delta t} \end{bmatrix}.$$

The process noise matrix is taken to be $Q_k = \text{diag}\{10^{-5}, 10^{-5}\}$. Measurements in the form of Cartesian position coordinates are generated from the targets at 1 [Hz] with a constant probability of detection of $p_D = 0.75$. If detected, measurements are corrupted with zero-mean additive Gaussian noise with standard deviation $\sigma_{x,y} = 0.1\,[\text{m}]$. Clutter is generated as a Poisson RFS with intensity $\kappa_{\text{c}}(z) = \lambda_{\text{c}} \mathcal{U}_{\mathbb{Z}}(z)$, where $\lambda_{\text{c}} = 3.0$.

To study the efficacy of the data-driven δ-GLMB filter, its performance is compared to the original δ-GLMB filter with the adaptive LMB birth process proposed in Reference 21. The computational complexity of each filter is controlled through the maximum allowed number of hypotheses, which is chosen as $J_{\max} = 500$. The adaptive LMB implementation additionally requires specification of a maximum birth target weight, which is chosen as $r_{B,\max} = 0.75$. A total of 500 Monte Carlo simulations are run, in which detectability, measurement noise, and clutter are randomly sampled. Target trajectories and times of birth are held constant across the runs. At each time step, state estimates are extracted from the multitarget posterior density using a suboptimal version of the

so-called "Marginal Multi-object Estimator," as presented in Reference 13. Using the positional components of the state estimates and the true target positions, the first-order optimal subpattern assignment (OSPA) metric[24] is computed with cutoff distance $c = 0.5\,[\text{m}]$ and averaged over the 500 runs, as shown in Figure 4a.

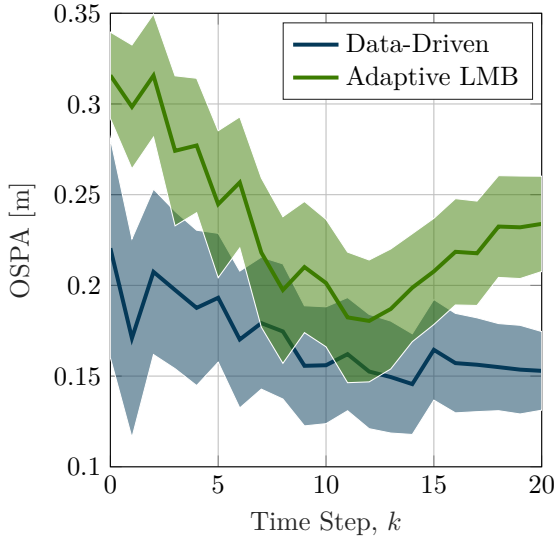

(a) Average first-order OSPA with cutoff $c = 0.5\,[\text{m}]$ over 500 trials. The standard deviation of the OSPA metric over the 500 trials is computed and its positive/negative deviation from the average is represented by the shaded regions.

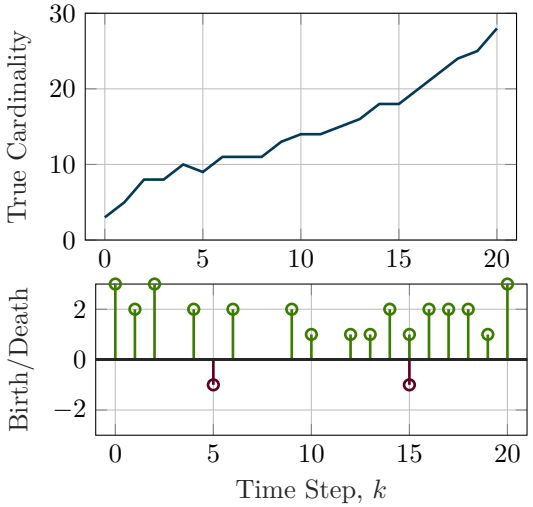

(b) True cardinality (top) and true number of target births and deaths (bottom) over time. Green stems represent the number of target appearances, and red stems represent the decrease in target number due to target death.

Figure 4: Average first-order OSPA and true target cardinality over time.

On average, lower OSPA values, and thus, higher accuracy estimates, are produced by the data-driven approach at every time step, as demonstrated in Figure 4a. Furthermore, the average estimation error of the data-driven filter trends downward over the simulation period, despite the steadily increasing number of visible targets, whereas the average estimation error given by the adaptive LMB approach trends upward after $k = 12$. The true total cardinality and birth/death cardinality shown in Figure 4b clearly reveal a correlation between the estimation performance and changes in target cardinality. Specifically, in the case of the adaptive LMB approach, all of the instances of significant accuracy improvement (in the form of drops in OSPA) coincide with instances when no targets are born, namely $k = 3, 5, 7, 8,$ and 11. To some extent, this correlation is expected due to the adaptive LMB method's inherent deferred birth initialization.

7.2 Example 2

Example 2 is similar to Example 1, except the simulation time, clutter rate, and measurement noise are increased. Measurements are corrupted with zero-mean additive Gaussian noise with standard deviation $\sigma_{x,y} = 0.25\,[\text{m}]$. Clutter is generated as a Poisson RFS with intensity $\kappa_{\text{c}}(z) = \lambda_{\text{c}}\mathcal{U}_{\mathbb{Z}}(z)$, where $\lambda_{\text{c}} = 5.0$. The simulation begins with three true targets and concludes with 102 true targets, with 116 true targets in total (14 target deaths). The true trajectories of all 116 targets are shown in Figure 5 and in Figure 6 with a single trial's detections overlayed.

In each of 500 Monte Carlo trials, detectability, measurement noise, and clutter are randomly sampled while the target trajectories and times of birth are held constant. The OSPA metric is averaged over the 500 trials and shown in Figure 7a for both methods. In terms of the OSPA multitarget miss distance, the data-driven δ-GLMB produces (on average) higher accuracy multitarget estimates at every time step. Note that trial-averaged OSPA results should be interpreted as a broad indication of filter importance, as relative performance could vary by

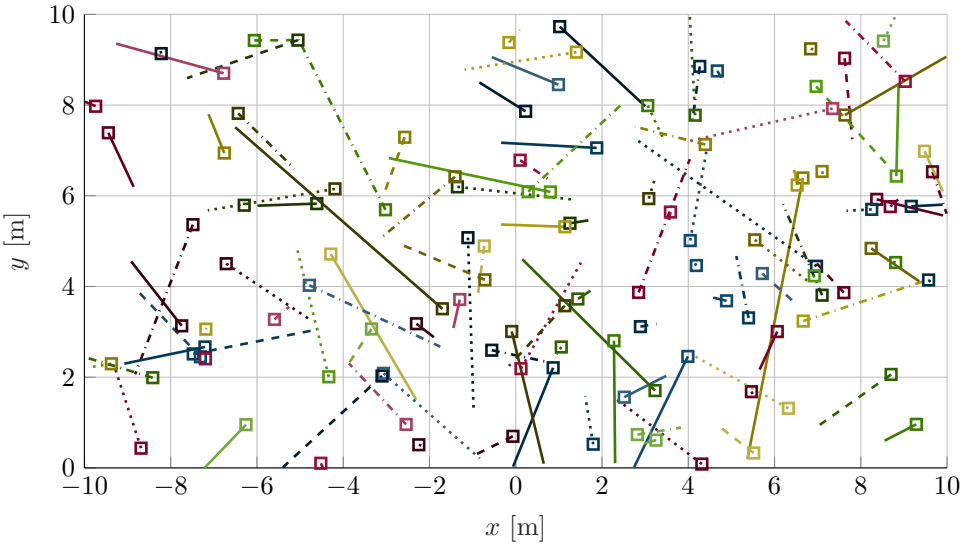

Figure 5: Simulated true motion. Starting locations are represented by square markers.

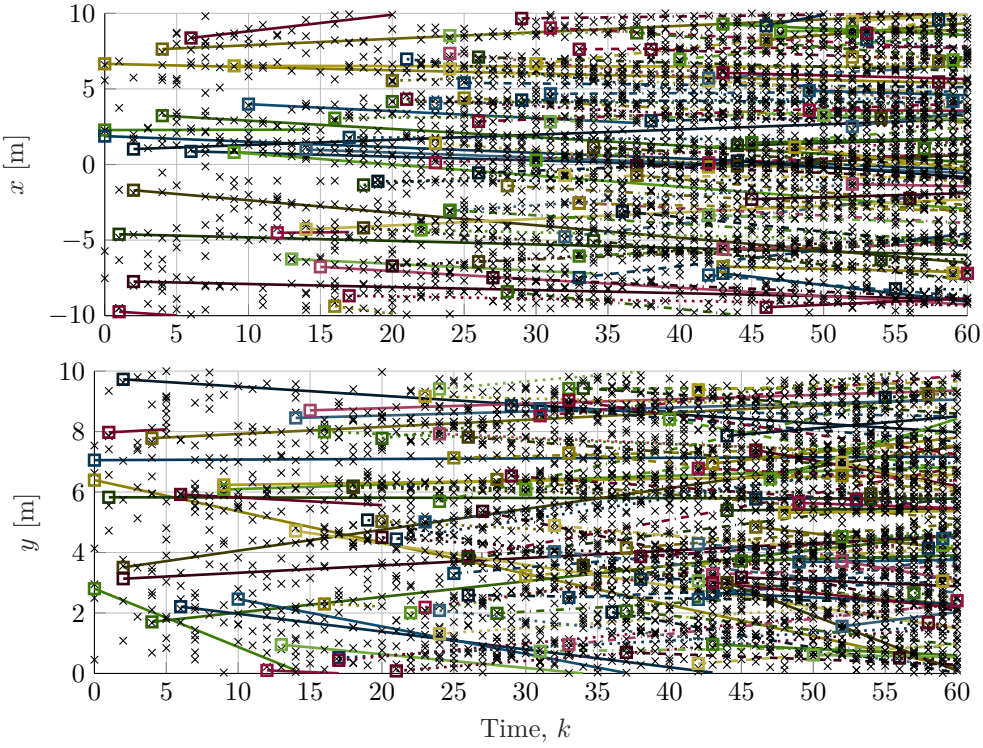

Figure 6: True position histories over time with overlayed measurements from a single Monte Carlo trial.

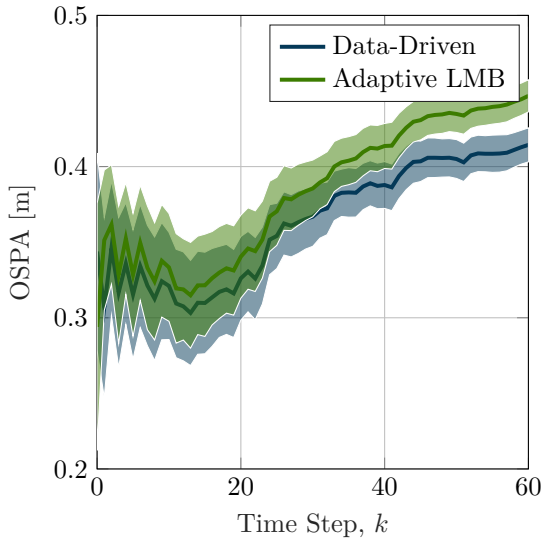

(a) Average first-order OSPA with cutoff $c = 0.5\,[\mathrm{m}]$ over 500 trials. The standard deviation of the OSPA metric over the 500 trials is computed and its positive/negative deviation from the average is represented by the shaded regions.

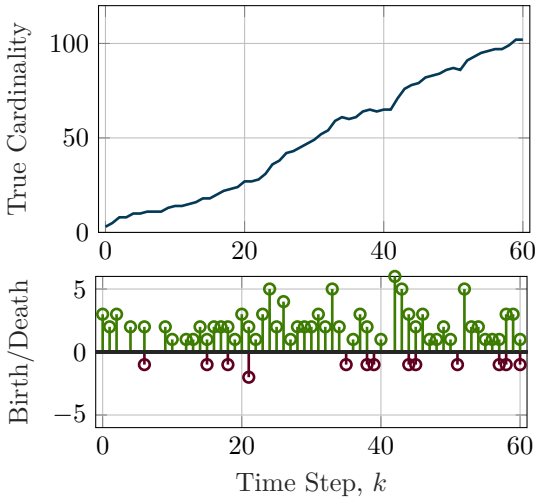

(b) True cardinality (top) and true number of target births and deaths (bottom) over time. Green stems represent the number of target appearances, and red stems represent the decrease in target number due to target death.

Figure 7: Average first-order OSPA and true target cardinality over time.

trial. In this example, the performance of both filters degrades significantly over time, as indicated by the rising OSPA values, which trend toward the cutoff distance $c = 0.5\,[\mathrm{m}]$.

Several adjustments could be made to potentially improve the performance of both filters in this example. Substitution of the suboptimal multitarget state extraction method with an optimal estimator would likely result in more accurate estimates and lower OSPA, although any optimal estimator would require more computational resources. Additionally, the maximum number of hypotheses $J_{\max}$ should be increased to better accommodate large numbers of targets, and more specifically, large numbers of measurements. While increasing $J_{\max}$ in this example would undoubtedly improve performance, the resulting error reduction is likely negligible when compared to other error sources. In particular, the combination of high spatial target density and relatively high measurement noise produces large data association errors. In fact, as suggested by Figure 6, the closest measurement to a given true target location is often a measurement generated by another target.

8. CONCLUSIONS

A variation of the standard δ-generalized labeled multi-Bernoulli (δ-GLMB) multitarget filter is derived under assumptions that facilitate the automatic initialization of new targets at the moment of their first detection. The resulting "data-driven" δ-GLMB filter differs from other adaptive birth approaches in that the birth initialization mechanism is an intrinsic part of the filter rather than an adaptation and avoids the introduction of bias. A key differentiation between the data-driven δ-GLMB and the standard δ-GLMB is the use of a new multitarget likelihood function that considers measurements from birth targets in addition to those originating from previously-detected "persistent" targets and clutter.

To evaluate the performance of the data-driven δ-GLMB filter, a simple tracking problem with multiple target appearances is simulated using synthetic measurement data. Two variants of the problem with differing levels of difficulty are demonstrated. For each variant of the tracking problem, a Monte Carlo analysis is performed using 500 trials with randomly-varying measurement noise, detectability, and clutter. In each trial, multitarget state estimates are extracted from the posterior density at each time step and used to compute the optimal subpattern assignment (OSPA) multitarget miss distance. A comparison between the data-driven δ-GLMB and

a similar adaptive birth approach is performed using OSPA values averaged over the Monte Carlo trials, and the data-driven δ-GLMB is shown to outperform the other method in both problem variants.

9. ACKNOWLEDGMENT

This research was funded by the Laboratory Directed Research and Development (LDRD) Program at Sandia National Laboratories. Sandia National Laboratories is a multimission laboratory managed and operated by National Technology and Engineering Solutions of Sandia, LLC, a wholly owned subsidiary of Honeywell International, Inc., for the U.S. Department of Energy's National Nuclear Security Administration under contract DE-NA0003525.

REFERENCES

[1] Bar-Shalom, Y., Willett, P. K., and Tian, X., [*Tracking and Data Fusion*], YBS publishing (2011).

[2] Blackman, S. S., "Multiple hypothesis tracking for multiple target tracking," *IEEE Aerospace and Electronic Systems Magazine* **19**(1), 5–18 (2004).

[3] Mahler, R. P., [*Statistical Multisource-Multitarget Information Fusion*], Artech House Boston (2007).

[4] Mahler, R. P., [*Advances in Statistical Multisource-Multitarget Information Fusion*], Artech House (2014).

[5] Mahler, R. P., "PHD filters of higher order in target number," *IEEE Transactions on Aerospace and Electronic Systems* **43**, 1523–1543 (October 2007).

[6] Vo, B.-N. and Ma, W.-K., "The Gaussian mixture probability hypothesis density filter," *IEEE Transactions on Signal Processing* **54**, 4091–4104 (Nov 2006).

[7] Vo, B.-T., Vo, B.-N., and Cantoni, A., "Analytic implementations of the cardinalized probability hypothesis density filter," *IEEE Transactions on Signal Processing* **55**, 3553–3567 (July 2007).

[8] Lin, L., Bar-Shalom, Y., and Kirubarajan, T., "Track labeling and PHD filter for multitarget tracking," *IEEE Transactions on Aerospace and Electronic Systems* **42**(3), 778–795 (2006).

[9] Nam, T. P., Huang, W., and Ong, S. H., "Maintaining track continuity in GMPHD filter," in [*2007 6th International Conference on Information, Communications and Signal Processing (ICICS)*], (2007).

[10] Pollard, E., Pannetier, B., and Rombaut, M., "Hybrid algorithms for multitarget tracking using MHT and GM-CPHD," *IEEE Transactions on Aerospace and Electronic Systems* **47**(2), 832–847 (2011).

[11] Vo, B.-T. and Vo, B.-N., "A random finite set conjugate prior and application to multi-target tracking," in [*Intelligent Sensors, Sensor Networks and Information Processing (ISSNIP), 2011 Seventh International Conference on*], 431–436 (2011).

[12] Vo, B.-T. and Vo, B.-N., "Labeled random finite sets and multi-object conjugate priors," *IEEE Transactions on Signal Processing* **61**(13), 3460–3475 (2013).

[13] Vo, B.-N., Vo, B.-T., and Phung, D., "Labeled random finite sets and the Bayes multi-target tracking filter," *IEEE Transactions on Signal Processing* **62**(24), 6554–6567 (2014).

[14] Mušicki, D. and Evans, R., "Joint integrated probabilistic data association: JIPDA," *IEEE Transactions on Aerospace and Electronic Systems* **40**(3), 1093–1099 (2004).

[15] Mahler, R. P., "Multitarget Bayes filtering via first-order multitarget moments," *IEEE Transactions on Aerospace and Electronic systems* **39**(4), 1152–1178 (2003).

[16] Vo, B. T., Vo, B. N., and Cantoni, A., "The cardinality balanced multi-target multi-Bernoulli filter and its implementations," *IEEE Transactions on Signal Processing* **57**(2), 409–423 (2009).

[17] Hoang, H. G., Vo, B.-T., and Vo, B.-N., "A generalized labeled multi-Bernoulli filter implementation using Gibbs sampling," *arXiv preprint arXiv:1506.00821* (2015).

[18] Vo, B.-N., Vo, B.-T., and Hoang, H. G., "An efficient implementation of the generalized labeled multi-Bernoulli filter," *IEEE Transactions on Signal Processing* **65**(8), 1975–1987 (2017).

[19] Ristic, B., Vo, B. T., Vo, B. N., and Farina, A., "A tutorial on Bernoulli filters: Theory, implementation and applications," *IEEE Transactions on Signal Processing* **61**(13), 3406–3430 (2013).

[20] Reuter, S., Meissner, D., Wilking, B., and Dietmayer, K., "Cardinality balanced multi-target multi-Bernoulli filtering using adaptive birth distributions," *Proceedings of the 2013 16th International Conference on Information Fusion* , 1608 – 1615 (2013).

[21] Lin, S., Vo, B.-T., and Nordholm, S. E., "Measurement driven birth model for the generalized labeled multi-Bernoulli filter," in [*2016 International Conference on Control, Automation and Information Sciences (ICCAIS)*], 94–99 (Oct 2016).

[22] Ristic, B., Clark, D., Vo, B. N., and Vo, B. T., "Adaptive target birth intensity for PHD and CPHD filters," *IEEE Transactions on Aerospace and Electronic Systems* **48**(2), 1656–1668 (2012).

[23] Houssineau, J. and Laneuville, D., "PHD filter with diffuse spatial prior on the birth process with applications to GM-PHD filter," in [*2010 13th International Conference on Information Fusion*], 1–8 (July 2010).

[24] Schuhmacher, D., Vo, B.-T., and Vo, B.-N., "A consistent metric for performance evaluation of multi-object filters," *IEEE Transactions on Signal Processing* **56**(8), 3447–3457 (2008).